Article, Author's Postprint

Naulin, Marie; Kortenhaus, Andreas; Oumeraci, Hocine

Reliability-Based Flood Defence Analysis in an Integrated Risk Assessment

Coastal Engineering Journal

Erstveröffentlichung in Coastal Engineering Journal,
No. 1 (2015), S. 1540005-[1-35].
Für eine korrekte Zitierbarkeit ist die Seitennummerierung der Originalveröffentlichung für jede Seite kenntlich gemacht. S. 1540005-1

Reliability-Based Flood Defense Analysis in an Integrated Risk Assessment

M. Naulin[a], A. Kortenhaus[b] and H. Oumeraci[c]

[a] Federal Waterways Engineering and Research Institute, Bundesanstalt für Wasserbau (BAW), Hamburg, Germany
marie.naulin@baw.de

[b] Faculty of Engineering and Architecture, Department of Civil Engineering, Ghent University, Belgium

[c] Department of Hydromechanics and Coastal Engineering, Leichtweiß-Institute for Hydraulic Engineering and Water Resources (LWI), Technische Universität Braunschweig, Germany

Received 13 June 2014, Accepted 6 February 2015, Published 13 April 2015

Failures of flood defenses have been one of the major reasons in the past leading to flooding of the hinterland behind flood defenses along rivers and at the sea. It is therefore inevitable to investigate the reliability of such defenses for extreme events as have occurred in the past and are discussed to happen more frequently in the future and due to climate changes. The first subproject in XtremRisK (SP 1) and the related papers in this issue [Gönnert, G. and Gerkensmeier, B. [2015] "A multi-method approach to develop extreme storm surge events to strengthen the resilience of highly vulnerable coastal areas," Coast. Eng. J., this special issue; Wahl, T. et al. [2015] "Statistical assessment of storm surge scenarios within integrated risk analyses," Coast. Eng. J., this special issue; Tayel, M. and Oumeraci, H. [2015] "A hybrid approach using hydrodynamic modelling and artificial neural networks for extreme storm surge prediction, Coast. Eng. J., this special issue] have investigated the components of storm surges and their statistical occurrence, also in relation to the wave parameters. These results can now be used as input for investigating the reliability of flood defenses and provide an overall failure probability for different types of defenses and different failure modes. This paper therefore summarizes the key findings of the "risk pathway" analysis of XtremRisK Subproject 2 (SP 2) which comprise a reliability analysis

Naulin, Kortenhaus, Oumeraci: Reliability-Based Flood Defense Analysis in an Integrated Risk Assessment. Coastal Engineering Journal, No. 1 (2015), S. 1540005-[1-35]. S. 1540005-2

and breach modeling of coastal and estuarine flood defenses using storm surge scenarios and sea states, including their occurrence probabilities provided by XtremRisK SP 1. The paper discusses the key results, the progress, and challenges in reliability analysis and breach modeling of flood defenses. The developed and advanced methods were applied to pilot sites in Hamburg (Elbe Estuary) and the Island of Sylt (North Sea). These pilot sites are mainly protected by linear flood defenses such as sea dikes, estuarine dikes, coastal dunes, and flood defense walls. Results have shown that under extreme conditions many dikes may fail simply from wave overtopping and even overflow but also from dike breaching due to the severe loading of the dike slopes when heavy overtopping and overflow occurs. The inflowing water volumes were calculated based on time-dependent water levels and then used for inundation modeling of the hinterland in Subproject 3 (SP 3) of XtremRisK. Furthermore, the limit state equations for wave overtopping and overflow had been adapted to time-dependent simulations. An importance factor was introduced for the probability of breaching of sea dikes leading to significantly different failure probabilities. The length effect considering the different homogeneous segments in the dike ring of Hamburg-Wilhelmsburg was estimated using an upper and lower bound approach showing the importance of the segmentation of the dike ring.

Keywords: Reliability analysis; flood defenses; failure modes; breach modeling; failure probability; time-dependent limit state equations.

1 Introduction

In the past, storm surges have led to failures of coastal flood assets which caused major damages and loss of life also along the European North Sea Coast, e.g. the North Sea flood of 1953 caused over 2,500 fatalities in The Netherlands and the United Kingdom and the North Sea flood of 1962 caused over 300 fatalities in Germany (Sönnichsen and Moseberg, 1997). As a result of enhanced construction of flood defense assets and further flood control measures, the performance of the flood defense system was improved. The improved flood defenses could even withstand higher storm surge water levels with less damage, e.g. the storm tides of 1976 and of 1981 with the highest high water levels measured to date at the North Sea coast.

However, in the coming decades it may be expected that the risk of flooding will increase as a result of the following trends: (i) the magnitude and intensity of floods are likely to increase [IPCC, 2013, Chap. 13] as a result of climate change (e.g. rising sea levels, increased extreme water levels and wave heights); (ii) there has been a noticeable increase in the number of people and economic assets located in flood risk zones [Schwartz, 2005]. Hence, the flood risks will continue to occur and may even increase considerably during the coming decades.

In order to assess, reduce and manage flood risk in Europe the European Commission established the Directive 2007/60/EC, also known as "EU Floods Directive", in 2007. The Directive requires member states to first perform a preliminary assessment by 2011 in order to identify the areas at risk of flooding. For the identified zones it is then required to produce flood hazard and flood risk maps by 2013 and to establish flood risk management plans by 2015. The Directive applies to river basins as well as coastal areas in the territory of the European Union.

Naulin, Kortenhaus, Oumeraci: Reliability-Based Flood Defense Analysis in an Integrated Risk Assessment. Coastal Engineering Journal, No. 1 (2015), S. 1540005-[1-35]. S. 1540005-3

In order to determine the flood risk, it is crucial to analyze the reliability of flood defense structures. For this reliability analysis, possible failure mechanisms are described by limit state equations (LSEs) z (z = R−S) comparing strength (R) and loading (S) of the flood defense elements [see e.g. CUR, 1990]. LSEs of coastal structures were examined in several projects such as PROVERBS [Oumeraci et al., 2001], ProDeich [Kortenhaus, 2003], and FLOODsite [Allsop et al., 2007].

Recent publications with respect to reliability of flood defenses have different emphases. Hall et al. [2003] performed a national-scale flood risk assessment. For a probabilistic analysis of defense resistance generic fragility curves were used which were based on simple classification and did not take explicit account for defense geometry, and other key parameters. A methodology for regional-scale flood risk assessment was developed by Gouldby et al. [2008]. Defense failures were represented through fragility curves. Two failure mechanisms were considered: piping and rear face erosion from overtopping. In the risk assessment and uncertainty analysis by Apel et al. [2004] the location of a possible breach was assumed at certain points. For the calculation of the (point-)failure probability of a levee, the failure mechanism of overtopping was calculated. The spatial variability of the levee geometry and the length effect of different long river stretches on the failure probability were not considered in that study. Apel et al. [2009] analyzed the influence of dike breaches on flood frequency distributions along rivers by a dynamic probabilistic model. In the inundation hazard assessment model by Vorogushyn et al. [2010] the modeling components for channel flow, dike breaching and hinterland inundation were dynamically coupled. Hence, an unsteady analysis of a flood wave that accounts for the dependence of the hydraulic load on river dikes at various locations along the reach was performed. For the probabilistic dike breach model three possible dike breach mechanisms were considered: overtopping, piping and slope microinstability. Furthermore, time-dependent effects in flood risk analysis were further analyzed by Buijs et al. [2009]. Several deterioration processes were incorporated in a reliability analysis based on multiple failure modes.

This overview shows that in the current literature very different approaches were used when deciding (a) how many and which LSEs should be included for which flood defense structure; (b) which model should be used to describe strength and resistance within the LSEs; (c) how to account for time-dependent processes both in assessing the relevant input parameters for the LSEs and the models themselves; and (d) in which way to consider the length of the flood defense segments in assessing the overall failure probability of the flood defenses (often called “length effect”). The focus of this study has therefore been laid upon the extensive use of LSEs for the different flood defenses on a very local scale, the variation of these LSEs during the storm event, and the discussion of the length effect.

Table 1 provides an overview of some key references dealing with the aforementioned issues, comparing the type of structure as well as the number and kind of LSE described. The number of LSE for each dike segment varies between 4 LSE and

Naulin, Kortenhaus, Oumeraci: Reliability-Based Flood Defense Analysis in an Integrated Risk Assessment. Coastal Engineering Journal, No. 1 (2015), S. 1540005-[1-35]. S. 1540005-4

Reference	Structure	Limit State Equations (LSE)	Remark
Voortman [2002]	Sea and estuary dikes	4 LSE (overflow and wave overtopping, failure of seaside revetment, piping, uplifting of landward clay layer)	Time dependency of processes is not considered LSE based on: TNO [1998], Hussaarts et al. [1999], Bligh [1910]
Kortenhaus [2003]	Sea and estuary dikes	25 LSE (overflow, wave overtopping, breach, sliding, revetment stability, wave impact, revetment uplift, velocity wave run-up, erosion grass cover on seaward slope, erosion clay cover on seaward slope, cliff erosion, deep slip of seaward slope, velocity overflow, velocity overtopping, erosion grass cover on landward slope, erosion clay cover on landward slope, infiltration, seepage, clay cover	Some time-dependent parameters are included in LSE (e.g. duration of storm surge (ts)), scenarios are described LSE based on: DIN 1054 [1996], Van der Meer [1998], DIN 4084 [1983], Richwien and Weißmann [1999], Kortenhaus and Oumeraci [2002], Sellmeijer [1988], De Mello [1975], INFRAM [2000] Only cross sections are considered, length of

		uplift at landward slope, deep slip of landward slope, full breach, dike top failure, piping, suffusion)	flood defenses not accounted for
Steenbergen and Vrouwenvelder [2003]	Dike ring	23 LSE (overflow/wave overtopping, deep slip, rupture/piping, damage of covers and erosion dike body, piping near structures, not-closed structure, dune erosion)	Some time-dependent parameters are included in LSE LSE based on: Bishop [1955], Sellmeijer [1988], Verheij [1997a], Verheij [1997b], Klein Breteler [1994], Lane [1935] Length of flood defenses considerd by segments of the same length

Table 1. Overview of existing literature and associated LSEs for sea dikes modified from Kortenhaus [2003].

Naulin, Kortenhaus, Oumeraci: Reliability-Based Flood Defense Analysis in an Integrated Risk Assessment. Coastal Engineering Journal, No. 1 (2015), S. 1540005-[1-35].
S. 1540005-5

Reference	Structure	Limit State Equations (LSE)	Remark
Zesch and Saucke et al. [2007]	River dike	10 failure processes described (overflow, wave overtopping, rupture, piping, settlement, micro-instability, erosion, sliding, macro-	Time dependency of processes is not considered LSE based on: Weijers and Sellmeijer, [1993]

		instability, failure in the area of a structure) 3 LSE (rupture, piping, settlement)	
Allsop et al. [2007]	Sea, estuary, and river dikes	Over 80 LSE for different structures, not only dikes and embankments	Some time-dependent parameters are included LSE based on all previous works
Vorogushyn [2009]	River dike	7 LSE (describing three most important failure mechanisms identified in fault tree) (overflow, piping (seepage, rupture, piping, critical pipe length), micro-instability of slope (seepage, micro-instability))	Some time-dependent parameters are included in LSE LSE based on: Apel et al. [2004], Merz [2006], Scheuermann [2005], Steenbergen and Vrouwenvelder [2003], Weijers and Sellmeijer [1993], CUR [1990]
Sch¨uttrumpf et al. [2009]	River dike	4 LSE (for dike failure) (overflow, wave overtopping, rupture, piping, seepage)	process chains are described, but time dependency of processes is not considered LSE based on: EurOtop [2007], Peter [2005], DIN 19712 [1997], Lane [1935] or Weijers and Sellmeijer [1993], Bardet and Tobita [2002]
Mai Van [2010]	Sea dike in Vietnam	10 LSE (overflow, wave overtopping, instability of armor unit, geo insta-	time dependency of processes is not considered LSE based on: Allsop

		bility of outer and inner slope, instability of toe protected element, excessive toe erosion, instability of toe structure, piping condition (rupture, piping))	et al. [2007], CUR [1990]

Table 1. (Continued)

Naulin, Kortenhaus, Oumeraci: Reliability-Based Flood Defense Analysis in an Integrated Risk Assessment. Coastal Engineering Journal, No. 1 (2015), S. 1540005-[1-35]. S. 1540005-6

25 LSE, depending on the author and the type of dike investigated. The most important failure modes, like wave overtopping and piping, are included in each reference, but sometimes using different models to describe strength and resistance in the LSEs.

The key objective of this paper is therefore to (a) find a consistent approach in which LSEs are used for flood defense structure; (b) find and possibly improve the best suitable model to assess the failure probability; (c) identify the most important failure modes/LSEs and include time-dependent analysis when needed; and (d) find a suitable way to address the length effect of the flood defense structures. This overall methodology will then be applied to two pilot sites where data are readily available and which can be identified as an open coast (Sylt Island) and an estuary (Hamburg), respectively. Furthermore, models should be applied and evaluated which describe the inflow boundary conditions for inundation modeling in the hinterland of flood defenses.

For this purpose, the paper first seeks to outline consistent methodology for a risk pathway approach (Sec. 2), then to provide a brief overview of the pilot sites and the available data (Sec. 3), to summarize the key results which have been achieved (Sec. 4) and finally to discuss these results (Sec. 5), also providing needs for clarification and further research.

2 Methodology

2.1 General approach

The key elements of the risk pathway analysis in the integrated risk analysis framework are shown in a flow chart in Fig. 1 which comprises a reliability analysis of coastal flood defenses and a breach modeling of sea dikes and coastal dunes. Based on the results of the "risk source analysis" [Gönnert and Gerkensmeier, 2015; Wahl et al., 2015; Tayel and Oumeraci, 2015], different extreme storm surge scenarios including their exceedance probabilities are used as input parameters for this study. It should be noted that this input was derived based on detailed multivariate extreme value methods in subproject 1 (SP1) of XtremRisK [see Wahl et al., 2015] the details of which will not be reproduced here. Further approaches, such as for example discussed in Wyncoll and Gouldby [2013], Lamb et al. [2010], and Heffernan and Tawn [2004] have also been considered in SP 1 and are not further considered here.

Results of this study were delivered to the "risk receptor analysis" [Ujeyl and Rose, 2015; Dassanayake et al., 2015; Burzel et al., 2015] and were later used to integrate all results within the "risk analysis framework" (Fig. 1), [Oumeraci et al., 2015]. Details of the reliability analysis, overtopping and overflow simulations, and the breach modeling are provided in the following subsections.

2.2 Reliability analysis

For the reliability analysis the following main steps were performed: (a) identification of flood defense segments in the aforementioned areas; (b) identification of relevant

Naulin, Kortenhaus, Oumeraci: Reliability-Based Flood Defense Analysis in an Integrated Risk Assessment. Coastal Engineering Journal, No. 1 (2015), S. 1540005-[1-35].

S. 1540005-7

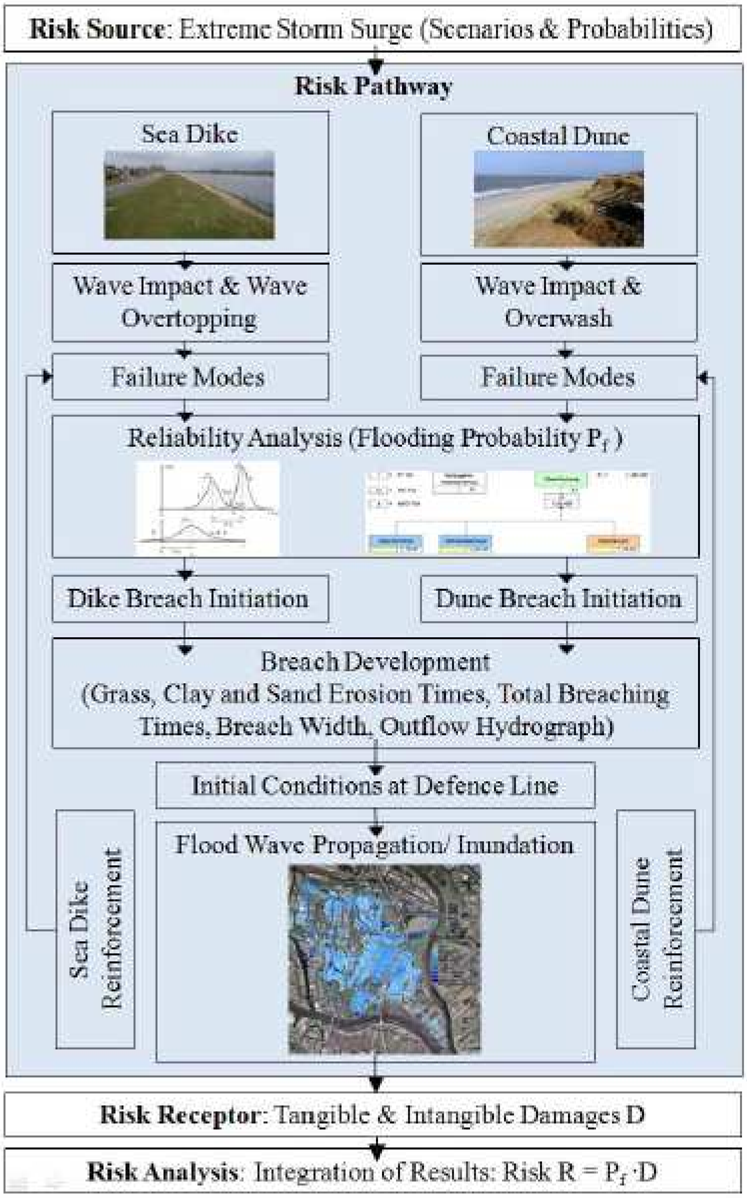

Fig. 1. Flow chart of risk pathways analysis in an integrated risk analysis framework [Naulin et al., 2012].

failure mechanisms and LSEs for each of these segments; (c) failure probability calculations; (d) combination of the different failure mechanisms by a fault tree analysis to calculate the flooding probability for a single flood defense element and the entire flood defense system. For the failure probability calculations, failure is defined as flooding of the hinterland which can be caused by non-structural failure such as overflow and wave overtopping, or structural failure such as dike breaching. For further use in this paper, probabilities are denoted as numbers in between 0 and 1 and referring to probabilities per year. Generally, these probabilities can be also referred to as return periods which can be calculated as the inverse of the probabilities.

Naulin, Kortenhaus, Oumeraci: Reliability-Based Flood Defense Analysis in an Integrated Risk Assessment. Coastal Engineering Journal, No. 1 (2015), S. 1540005-[1-35]. S. 1540005-8

As mentioned before, the input for this analysis were exceedance probabilities of extreme storm surges which were determined by a multivariate statistical approach based on Copula functions [see Wahl et al., 2015]. This approach was used to both determine the occurrence probabilities of storm surges in the past and to generate artificial extreme storm surges, including the temporal development of water levels. Existing data were then used to provide wave parameters for a storm surge of this occurrence probability. This scenario approach was selected to better allow for inclusion of time-dependent LSEs like wave overtopping and breach modeling (see Sec. 4.1), but also for the inundation modeling of the hinterland [Ujeyl and Rose, 2015]. The results of the failure probabilities P_f from this study were therefore combined with the exceedance probabilities P_e of the storm surge scenarios. Hence, the conditional failure probability $P_{f,}$ cond. for each extreme storm surge scenario (characterized by an occurrence probability P_e and a time series of water level and wave heights and periods) was eventually calculated by:

$$P_{f,cond.} = P_e \cdot P_f \,. \tag{1}$$

For the reliability analysis of the flood defenses, a probabilistic approach by taking into account the uncertainties of input parameters and models was applied. For this purpose, different failure modes described by relevant LSEs were analyzed:

$$z = R - S, \tag{2}$$

where R denotes the resistance, S the stress or loading and z the resulting limit state of the mechanism in question. Due to the uncertainties usually associated with stress and resistance parameters and due to the sometimes very high complexity of these LSEs, obtaining the failure probabilities is very often quite complex. Within this paper all calculations have been performed using a level III approach (Monte Carlo simulations).

Flood defense lines within the pilot sites were divided into segments with similar or identical characteristics (homogeneous segments, see Sec. 3 and Appendix A for more details). For these segments and the related flood defenses, all failure mechanisms were examined based on the results of previous projects such as FLOODsite [Allsop et al., 2007] and ProDeich [Kortenhaus, 2003]. Results of this approach are shown in Sec. 4.1 and will be discussed in Sec. 5.

For each segment the aforementioned failure mechanisms were organized in a fault tree. The structure of the fault tree represents the different chains of events leading to an overall failure of the flood defense structure (top event) which was defined in this study as flooding of the hinterland. Flooding of the hinterland can be caused by non-structural failure such as overflow and wave overtopping, or structural failure such as dike breaching. The generic structure of the fault tree combining LSEs of sea dikes and coastal dunes are shown in Fig. 2. For the failure probability calculations software tools such as the FLOODsite software tool RELIABLE [Van Gelder et al., 2008] or ProDeich [Kortenhaus, 2003] were adapted and applied.

Naulin, Kortenhaus, Oumeraci: Reliability-Based Flood Defense Analysis in an Integrated Risk Assessment. Coastal Engineering Journal, No. 1 (2015), S. 1540005-[1-35]. S. 1540005-9

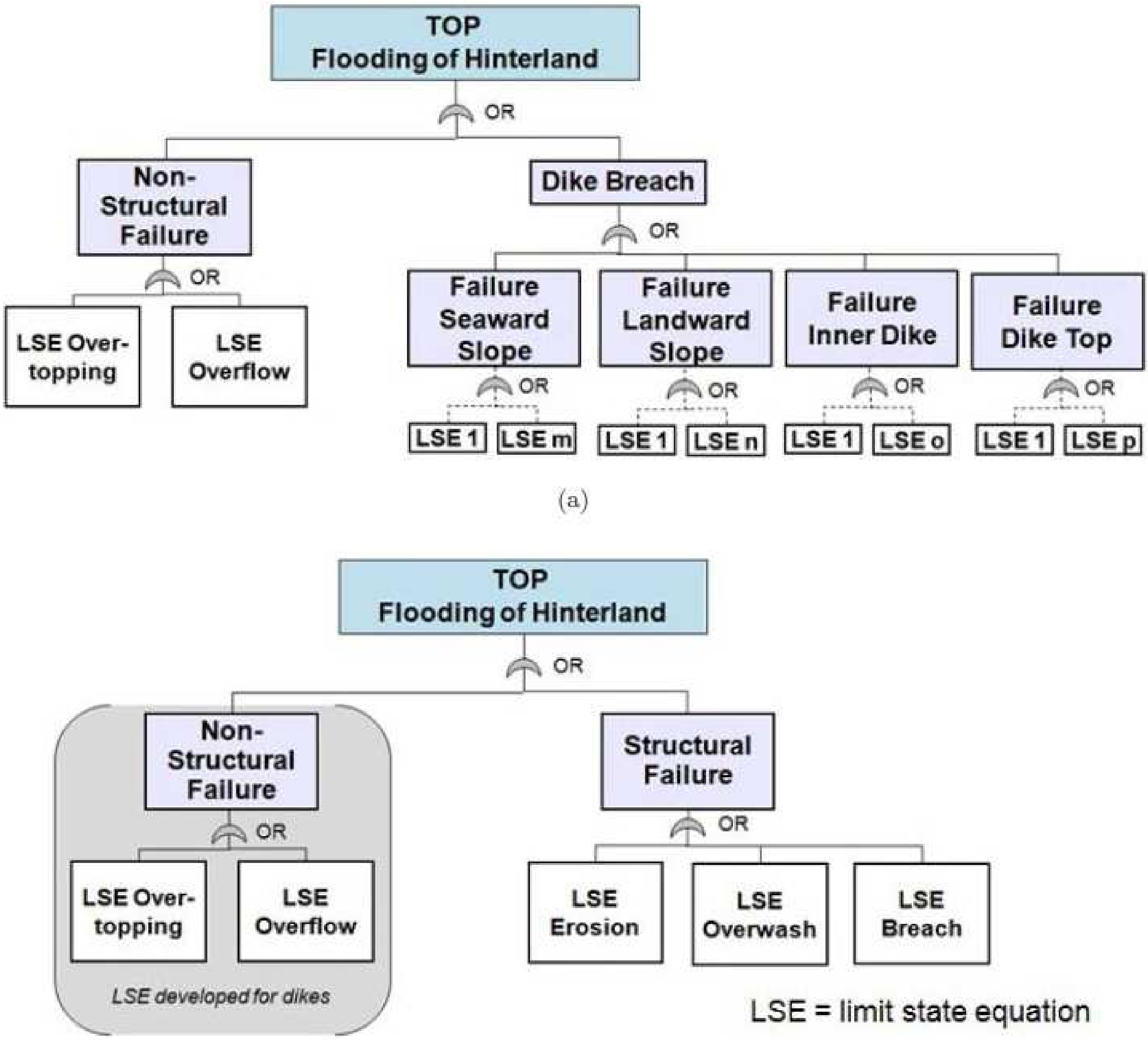

Fig. 2. Generic fault tree combing LSE of (a) sea dikes and (b) coastal dunes [Naulin et al., 2012].

2.3 Wave overtopping and overflow

Very high discharges over the flood defenses were used as boundary conditions for the inundation simulations of the hinterland and were determined by wave overtopping and/or overflow calculations. For this purpose, the time-dependent conditions of water level and wave parameters at the toe of the defenses were considered as input data using time series of about 28 h with time steps of 15 min.

The combined overtopping and overflow discharges were calculated according to two approaches (i) for most segments of the flood defense line, i.e. simple sloping and vertical structures, the discharges were calculated using existing weir formulae and wave overtopping formulae [Bleck et al., 2000; EurOtop, 2007]; and (ii) for specific cross sections of dikes a numerical model was applied [Tuan and Oumeraci, 2010]. The output of these models was time-dependent discharges (resolution of 15min) for

Naulin, Kortenhaus, Oumeraci: Reliability-Based Flood Defense Analysis in an Integrated Risk Assessment. Coastal Engineering Journal, No. 1 (2015), S. 1540005-[1-35]. S. 1540005-10

each segment of the flood defenses. Only this method, together with the scenariobased approach of extreme storm surges, allowed for sufficient details of the input boundary conditions for the inundation modeling.

2.4 Breach modeling

The breach modeling was performed for specific cross-sections of dikes where the results of the reliability analysis indicated that the probabilities of breaching were very high. For the different causes of breach initiation, there are different breaching models available, e.g. breaching initiated on the landside by wave overtopping and overflow [D'Eliso et al., 2006; Tuan and Oumeraci, 2012] as well as breaching initiated on the seaside by breaking wave impacts [Stanczak and Oumeraci, 2012]. Depending on the loading conditions (wave overtopping/overflow or breaking wave impacts) and thus depending on the breach initiation (landside or seaside) one of the aforementioned breaching models was applied to the specific segment. As boundary conditions for breach modeling the water levels and wave parameters of the extreme storm surge scenarios were applied. The parameters were determined at the toe of the sea dike using hydrodynamic models and wave models. Similarly to the wave overtopping and overflow calculations, the time-dependent results of the breach model were used as boundary conditions for the inundation modeling of the hinterland.

Furthermore, the erosion of coastal dunes due to storm surges was modeled by applying the model Unibest-DE [Steetzel, 1993]. Unibest-DE uses time-dependent input hydraulic boundary conditions such as water levels and waves and calculates the time-dependent cross-shore equilibrium of sand dunes. From the final profile at the end of the extreme storm surge criteria were developed to define the progress of erosion or whether the dune has breached.

3 Pilot Sites and Data

The pilot sites, Hamburg and Sylt, are located in the northern part of Germany [Fig. 3(a)]. As an example for an open coast, the Island of Sylt in the North Sea is analyzed whereas the Elbe Estuary of the city of Hamburg serves as an example for an estuarine urban area. However, the methods developed in XtremRisK are generic enough to be applied also to other coastal and estuarine areas at risk.

Typical subareas with characteristic properties for the two pilot sites were selected. In Hamburg, the subareas of Wilhelmsburg, Polder Hamburg Süd, and a part of the city centre were selected for the detailed study [Fig. 3(b)]. For Sylt Island, the subareas of Hörnum and Westerland were selected for the detailed study [Fig. 3(c)].

Therefore, for both pilot site areas, data describing the characteristics of the flood defense line were required. For the identified subareas of the pilot sites, a detailed description and parameterization of all flood defenses were performed (see

Naulin, Kortenhaus, Oumeraci: Reliability-Based Flood Defense Analysis in an Integrated Risk Assessment. Coastal Engineering Journal, No. 1 (2015), S. 1540005-[1-35]. S. 1540005-11

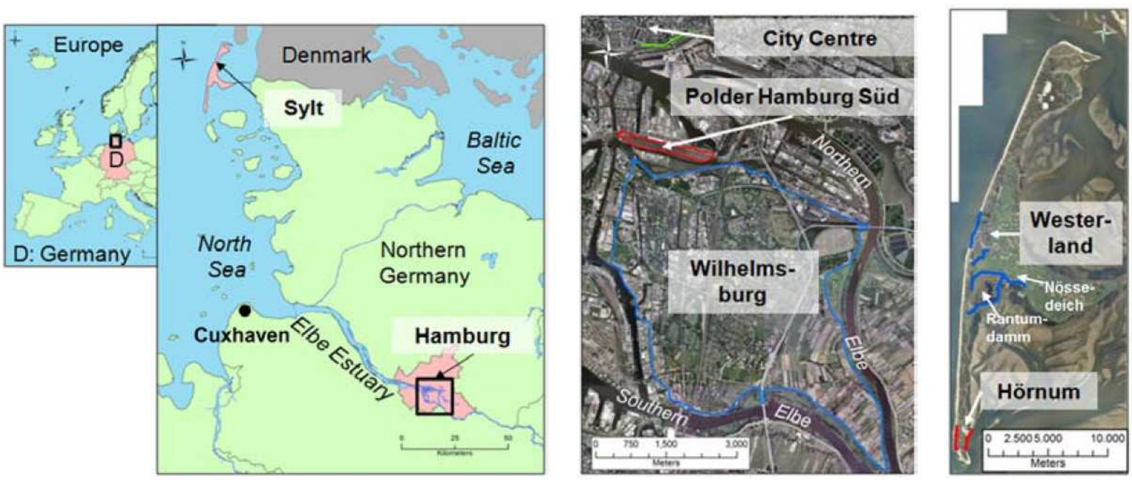

Fig. 3. Pilot sites selected for this study in XtremRisK location in (a) Germany; (b) Hamburg and (c) Sylt Island.

Appendix A). This analysis was based on inventory documents, geotechnical reports, digital terrain models, and field studies. The survey and data collection where performed in close cooperation with local port and coastal defense authorities of the pilot sites (i.e. Schleswig-Holstein's Government-Owned Company for Coastal Protection, National Parks and Ocean Protection (LKN-SH), Hamburg Port Authority (HPA) and Agency of Roads, Bridges and Waters Hamburg (LSBG)).

The flood defense lines in both areas were split into "homogeneous" segments according to similar characteristics such as type of structure, geometric and geotechnical parameters as well as hydraulic conditions (for details see Appendix A). The result of this segmentation is exemplarily shown in Fig. 4 for the subarea Hamburg- Wilhelmsburg.

The main part of the flood defense line, i.e. 19 km out of 24 km, consisted of dikes. The dikes were built of a sand core, a clay layer with a thickness of up to 2.0m and a grass cover on top. The crown heights of the dikes varied from 7.80 mNHN to 8.35 mNHN and in general the outer and inner slopes were 1 in 3.

Overall the flood defense line around Hamburg-Wilhelmsburg was divided into 94 segments. Out of these segments a total number of 71 segments were dikes and 7 segments were walls. Furthermore, there were 16 point structures such as gates.

4 Results

4.1 Reliability

analysis In this section, the results of the reliability analysis of the linear flood defense elements are summarized and discussed. Results were achieved by applying a total

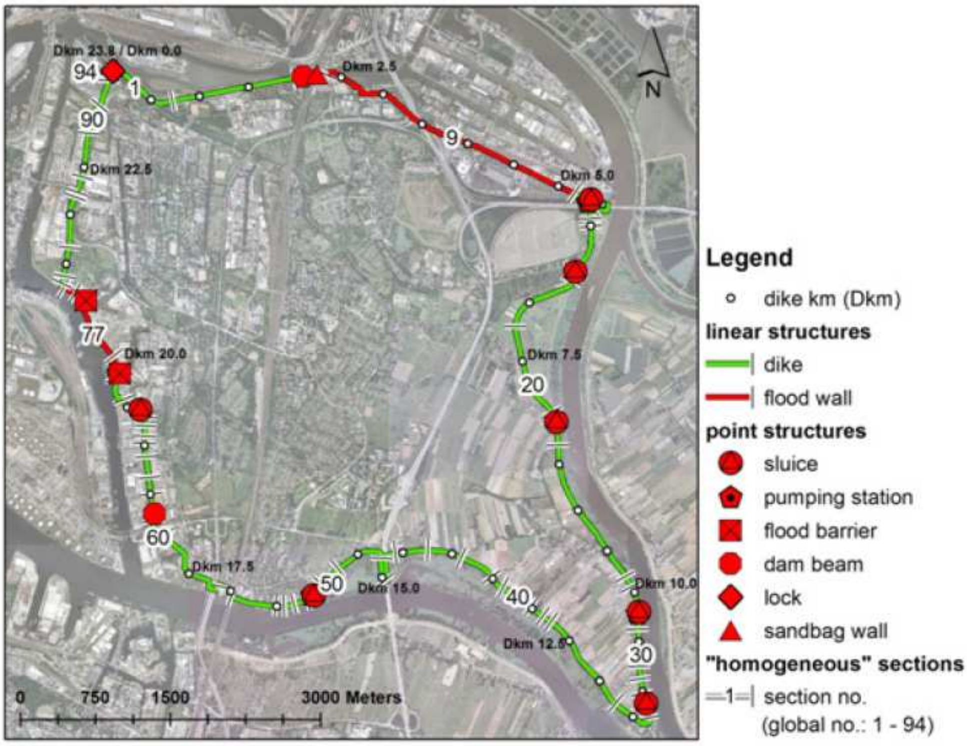

Fig. 4. Segments of the flood defense line of the study subarea Wilhelmsburg, Hamburg.

of 35 failure mechanisms, i.e. 22 LSEs for sea dikes, 5 LSEs for coastal dunes and 8 LSEs for flood defense walls. An overview of the considered LSEs is given in Table 2.

As stated earlier, most of the LSEs for this study were taken from literature. However, some of the LSEs were not readily available but had to be adapted to the situation within the pilot site areas. These LSEs are marked by an asterisk in Table 2 and needed to be composed of several LSEs. For example, the "sliding of clay layer" on the landward side of a dike was initially described by a LSE comparing the shear forces and the resistant forces of the clay layer. However, the shear forces only occur when wave overtops the dike for a certain time. This condition has been added to the LSE to achieve a better description of the limit states.

It should however be noted that most of the LSEs were not time-dependent approaches as indicated in the column "f(t)" in Table 2. The drawbacks associated to this limitation are discussed in the following in more detail. The results of the failure probabilities of the top event, i.e. flooding of the hinterland, reach very high values with $P_f = 1.0$ for the different storm surge scenarios.

The relevant failure mechanisms were determined to be wave overtopping and overflow due to the very high water levels for the extreme storm surge scenarios and the relatively low allowable rate for wave overtopping or overflow which was set to q = 0.5 l/(sm) for this study. At this point, it should be noted that exceeding this limit must of course not necessarily result in a functional failure of the flood defense system. However, the allowable overtopping rate is usually set to low values to avoid

Naulin, Kortenhaus, Oumeraci: Reliability-Based Flood Defense Analysis in an Integrated Risk Assessment. Coastal Engineering Journal, No. 1 (2015), S. 1540005-[1-35]. S. 1540005-13

No.	LSE Name	f(t)	Comparison of . . .	Unit
Sea	Dike/Estuary Dike			
Non-structural failure of dikes				
1	Overflow (functional failure)	-	overflow rates (or energy heights)	$m^3/s/m$ or m/m
2	Wave overtopping (functional failure)	-	overtopping rates (or freeboards)	$m^3/s/m$ or m/m
Failure of seaward slope of dikes				
3	Velocity wave run-up	-	wave velocities	m/s
4	Wave driven erosion	x	times	h
5	Cliff erosion by wave impact	-	times	h
6	Cliff erosion by wave impact	-	times	h
7	Erosion of revetment armor (rock)	-	stone diameters	m
8	Uplift of the revetment	-	forces of revetment elements	kN/m
9	Deep slip (Bishop)	-	moments of single Bishop's slices	kNm

Failure of landward slope of dikes				
10	Overflow velocity	-	overflow velocities	m/s
11	Wave overtopping velocity	-	wave overtopping velocities	m/s
12	Erosion by overflow/wave overtopping	-	times	h
13	Sliding of clay layer*	-	times and forces	h and kN
14	Clay uplift*	-	times and forces	h and kN
15	Deep slip (Bishop)	-	moments of single Bishop's slices	kNm
16	Partial breach	x	times	h
Sliding and internal erosion of dikes				
17	Sliding of dike with clay cover	-	forces	kN/m²
18	Piping*	-	times and pressure gradient	h and –
19	Matrix erosion*	-	times and sediment diameter	h and mm
Failure of dike top				
20	Erosion inner slope and dike top failure*	x	times and moments of Bishop's slices (sand)	h and kNm
21	Sliding inner slope and dike top failure*	x	times, forces and moments of single Bishop's slices (sand)	h, kN and kNm
22	Clay uplift inner slope and dike top	x		

	failure*			

Naulin, Kortenhaus, Oumeraci: Reliability-Based Flood Defense Analysis in an Integrated Risk Assessment. Coastal Engineering Journal, No. 1 (2015), S. 1540005-[1-35]. S. 1540005-14

No.	LSE Name	f(t)	Comparison of …	Unit
Coastal Dune				
Non-structural failure of coastal dunes				
1	Overflow (functional failure)	-	overflow rates (or energy heights)	$m^3/s/m$ or m/m
2	Wave overtopping (functional failure)	-	overtopping rates (or freeboards)	$m^3/s/m$ or m/m
Failure of seaward slope of coastal dunes				
3	Erosion	x	width of dune and erosion depth	m
Failure of landward slope of coastal dunes				
4	Overwash	-	overwash rates	$m^3/s/m$
5	Breaching	-	width of dune and breach width	m
Flood Defense Wall				
Non-structural failure of walls				
1	Overflow (functional failure)		overflow rates (or energy heights)	$m^3/s/m$ or m/m

2	Wave overtopping (functional failure)	-	overtopping rates (or freeboards)	$m^3/s/m$ or m/m
Structural failure of flood defense walls				
3	Deep slip (Bishop)	-	moments of single Bishop's slices	kNm
4	Overturning	-	moments	kNm
5	Piping	-	water level difference	m
6	Hydraulic heave	-	shear stress	kN/m^2 m
7	Failure of drainage	-	drainage rate	$m^3/s/m$
8	Bending	-	bending stiffness	kNm
*Composed of several LSE.				

Table 2. (Continued)

any damage to the flood defenses. This is a conceptual mismatch with the entirely functional LSE here where only the amount of water entering the hinterland is of importance. Therefore, two improvements were implemented here, which were to take (a) the time-dependent overflow and wave overtopping rate and (b) the resulting total flood volume into account. Details of these approaches are discussed later in this paper (Secs. 4.2 and 5.2). The results of the conditional failure probabilities for the storm surge scenarios in Hamburg and Sylt are presented in Tables 3 and 4, respectively, along with the exceedance probabilities and storm surge parameters [see Gönnert and Gerkensmeier, 2015; Wahl et al., 2015]. In Tables 3 and 4 the peak water level and the fullness (i.e. storm surge intensity) for different extreme storm surge scenarios are given. Furthermore, the associated univariate exceedance probability for the peak water level $P_{e,Peak}$ and the fullness $P_{e,fullness}$ as well as the bivariate exceedance probability $P_{e,bivariate}$ (water level and fullness) are provided. For the case of Hamburg (Table 3) the discharge of the Elbe river and associated exceedance probability $P_{e,Discharge}$ and trivariate exceedance probability $P_{e,Hamburg}$

Naulin, Kortenhaus, Oumeraci: Reliability-Based Flood Defense Analysis in an Integrated Risk Assessment. Coastal Engineering Journal, No. 1 (2015), S. 1540005-[1-35]. S. 1540005-15

Location	Scenario:	HH_XR2010A	HH_XR2010B	HH_XR2010C	HH_XR2010A-90
Cuxhaven	Peak water level [cmNHN]	610	531	650	530
	fullness [–]	537	770	767	449
	$P_{e,peak}$ [1/a] (univariate)	$3.17\ 10^{-4}$	$7.20 \cdot 10^{-3}$	$4.27 \cdot 10^{-6}$	$7.45 \cdot 10^{-3}$
	$P_{e,fullness}$ [1/a] (univariate)	$1.30 \cdot 10^{-2}$	$3.24 \cdot 10^{-6}$	$3.71 \cdot 10^{-6}$	$1.23 \cdot 10^{-1}$
	P_e [1/a] (bivariate)	$3.09 \cdot 10^{-4}$	$3.24 \cdot 10^{-6}$	$2.12 \cdot 10^{-6}$	$7.10 \cdot 10^{-3}$
Hamburg	discharge Elbe river [m3/s]	3600	3600	3600	2200
	$P_{e,Discharge}$ [1/a]	$2.50 \cdot 10^{-2}$	$2.50 \cdot 10^{-2}$	$2.50 \cdot 10^{-2}$	$3.33 \cdot 10^{-1}$
	Pe [1/a] (trivariate)	$7.72 \cdot 10^{-6}$	$8.09 \cdot 10^{-8}$	$5.30 \cdot 10^{-8}$	$2.36 \cdot 10^{-3}$
Wilhelmsburg	P_f	1.0	1.0	1.0	1.0
	P_f (no overtopping)	$4.4 \cdot 10^{-1}$	$5.4 \cdot 10^{-1}$	n.a.	negligible
	$P_{f,cond}$ [1/a]	$7.72 \cdot 10^{-6}$	$8.09 \cdot 10^{-8}$	$5.30 \cdot 10^{-8}$	$2.36 \cdot 10^{-3}$

Table 3. Storm surge scenarios and conditional failure probabilities in Hamburg.

Location	Scenario	SY_XR2010A	SY_XR2010B	SY_XR2010C	SY_XR2010A-95
Hörnum (East)	peak water level [cmNHN]	513	450	489	419
	fullness [–]	574	608	559	477
	$P_{e,peak}$ [1/a] (univariate)	$5.47 \cdot 10^{-6}$	$3.73 \cdot 10^{-3}$	$4.63 \cdot 10^{-4}$	$1.37 \cdot 10$ -2
	$P_{e,fullness}$ [1/a] (univariate)	$3.76 \cdot 10^{-4}$	$7.24 \cdot 10^{-5}$	$7.43 \cdot 10^{-4}$	$1.52 \cdot 10^{-2}$
	P_e [1/a] (bivariate)	$5.38 \cdot 10^{-6}$	$7.09 \cdot 10^{-5}$	$3.06 \cdot 10^{-4}$	$7.85 \cdot 10^{-3}$
Westerland	P_f	1.0	1..0	1.0	1.0
	$P_{f,cond}$ [1/a] (bivariate)	**$5.38 \cdot 10^{-6}$**	**$7.09 \cdot 10^{-5}$**	**$3.06 \cdot 10^{-4}$**	**$7.85 \cdot 10^{-3}$**
	P_f	1.0	1.0	1.0	1.0
	$P_{f,cond}$ [1/a] (bivariate)	$5.38 \cdot 10^{-6}$	$7.09 \cdot 10^{-5}$	$3.06 \cdot 10^{-4}$	$2.49 \cdot 10^{-5}$

Table 4. Storm surge scenarios and conditional failure probabilities at Sylt Island

(water level, fullness, discharge) are shown. Moreover, the failure probabilities for flooding P_f and failure without overtopping $P_{f,no\text{-}overtopping}$ are presented. Finally, the conditional failure probabilities $P_{f,cond}$ (exceedance of storm surge and reliability of flood defense system) are stated.

For both pilot sites the storm surge scenarios "A" have extremely high peak water levels (above the current design water level), the scenarios "B" have high

Naulin, Kortenhaus, Oumeraci: Reliability-Based Flood Defense Analysis in an Integrated Risk Assessment. Coastal Engineering Journal, No. 1 (2015), S. 1540005-[1-35]. S. 1540005-16

intensities (fullness) and the scenarios “C” have both extremely high peak water levels and high intensities.

As mentioned before, the dominant failure mechanisms were identified as nonstructural failure such as wave overtopping and overflow due to the extreme storm surge scenarios with very high water levels compared to the crown height of the flood defenses. For the case of Hamburg-Wilhelmsburg there were large stretches along the defense line where the overtopping discharges exceeded the allowable rate of 0.5 l/s/m. If this LSE is not considered, the flooding probability would not reduce significantly in the case of the extreme storm surges HH_XR2010A to HH_XR2010C due to the extreme overtopping and overflow discharges. However, in the case of the storm surge HH_XR2010A-90 with a significantly reduced water level the probability of dike breaches is insignificant and hence the overall probability is negligible. This will be further discussed below.

Taking the aforementioned high flooding probabilities into consideration, the conditional failure probability mainly depends on the exceedance probability of the storm surge scenarios P_e, so that e.g. the conditional failure probability $P_{f,cond.}$ results to $7.72 \cdot 10^{-6}$ per year for the storm surge scenario HH_XR2010A. The results show two principal learning lessons from these extreme scenarios:

• The exceedance probability of such extreme events is extraordinary small, the maximum (not considering the case with reduced water levels) being $P_e = 7.72 \cdot 10^{-6}$ for the storm surge HH_XR2010A for Hamburg and $P_e = 3.06 \cdot 10^{-4}$ for the storm surge SY_XR2010C for Sylt;

• If these storm surges occur the flood defenses will not be able to maintain their function and water will flow into the hinterland. The failure probabilities of the flood defenses (without considering overtopping) suggest that this will not necessarily lead to failure of the defenses itself although breaching is also likely under these severe conditions.

However, the latter point shows that it is of great importance to further analyze the structural stability of the flood defenses in more detail. A dike breach leads to extreme discharges and very high velocities of the flood wave propagation and hence a breach represents severe consequences for the hinterland. In order to analyze the structural stability of dikes, the results of the failure probabilities of the failure mechanisms leading to a dike breach (no “functional failure modes”) were examined. In the following sections the results are exemplarily shown for the storm surge scenario HH XR2010A for the dike segments of Wilhelmsburg, Hamburg.

Figure 5(a) shows the failure probabilities of the inner slope for all dike segments. For most dikes the probabilities of failure of the inner dike slope are rather low ($P_f = 1.0 \cdot 10^{-4}$). Only in some areas higher values (between $P_f = 1.0 \cdot 10^{-2}$ and $P_f = 1.0 \cdot 10^{-3}$) were calculated. These dike segments were then identified as weak spots since they had less resistant inner slopes or were exposed to more severe

Naulin, Kortenhaus, Oumeraci: Reliability-Based Flood Defense Analysis in an Integrated Risk Assessment. Coastal Engineering Journal, No. 1 (2015), S. 1540005-[1-35]. S. 1540005-17

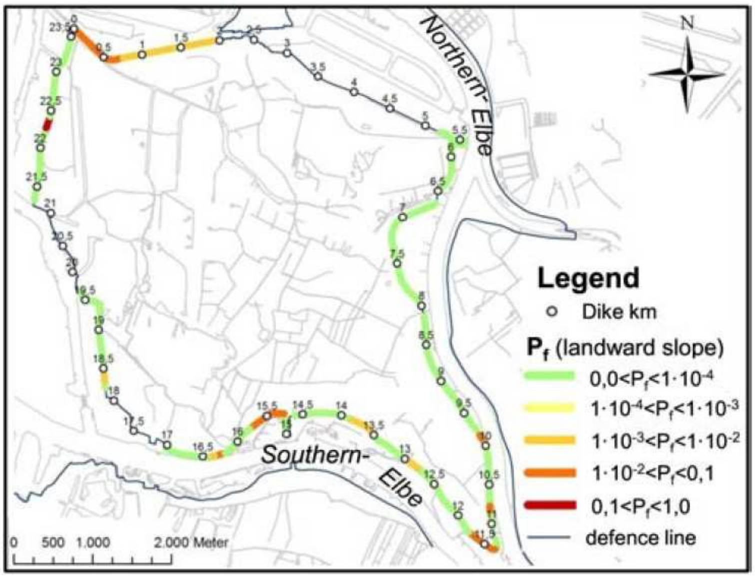

(a)

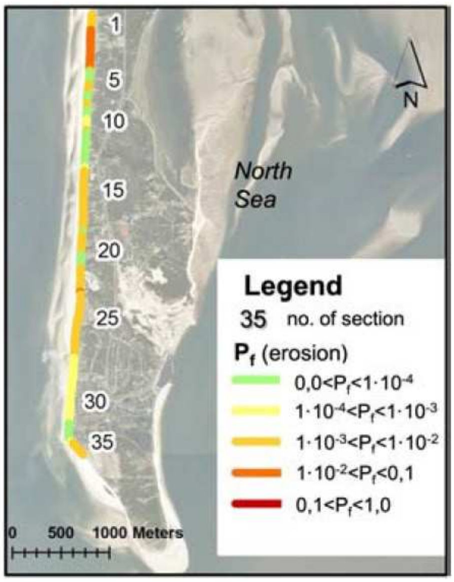

(b)

Fig. 5. Results of the two case studies: (a) Failure probabilities of dike breach initiated from a failure of the landward slope for dike segments in Wilhelmsburg, Hamburg; (b) Failure probabilities of erosion of coastal dunes in Hörnum, Sylt.

hydraulic loading. Breach modeling has been applied to these "weaker" segments as described in the next subsection.

Furthermore, the stability of the coastal dunes at Sylt Island was analyzed. In the following, the results of the failure probabilities of the coastal dunes of the west side of Hörnum are exemplarily given for the storm surge scenario SY_XR2010A. "Erosion" was determined as the dominating failure mechanism. For the LSE of erosion failure probabilities up to $P_f = 4.2 \cdot 10^{-2}$ (Sec. 2) were calculated. The results of all 35 dune segments are summarized in Fig. 5(b).

The results of the probability of flooding were delivered for risk integration (Dassanayake et al., 2015; Burzel et al., 2015). Moreover, the fault tree analysis allowed determining the probability of breaching of dunes and dikes and gave an indication of the causes of breach initiation, e.g. wave impact on seaward slope or overtopping on landward slope.

4.2 Wave overtopping and overflow

The results of the modeling of wave overtopping and/or overflow are presented in this section using the example of Wilhelmsburg, Hamburg. The discharge rates were determined for all identified segments of the flood defense line (see Fig. 4). The crown heights of the flood defense segments in comparison to the peak water level of the different storm surge scenarios are presented in Fig. 6. As it can be seen, segment 9, i.e. a flood defense wall with a length of 2870m and a crown height of 7.70mNN represents a weak point (e.g. for the storm surge scenario HH_XR2010A maximum values of discharges of up to 0.250m^3/s/m were calculated for this segment).

Naulin, Kortenhaus, Oumeraci: Reliability-Based Flood Defense Analysis in an Integrated Risk Assessment. Coastal Engineering Journal, No. 1 (2015), S. 1540005-[1-35]. S. 1540005-18

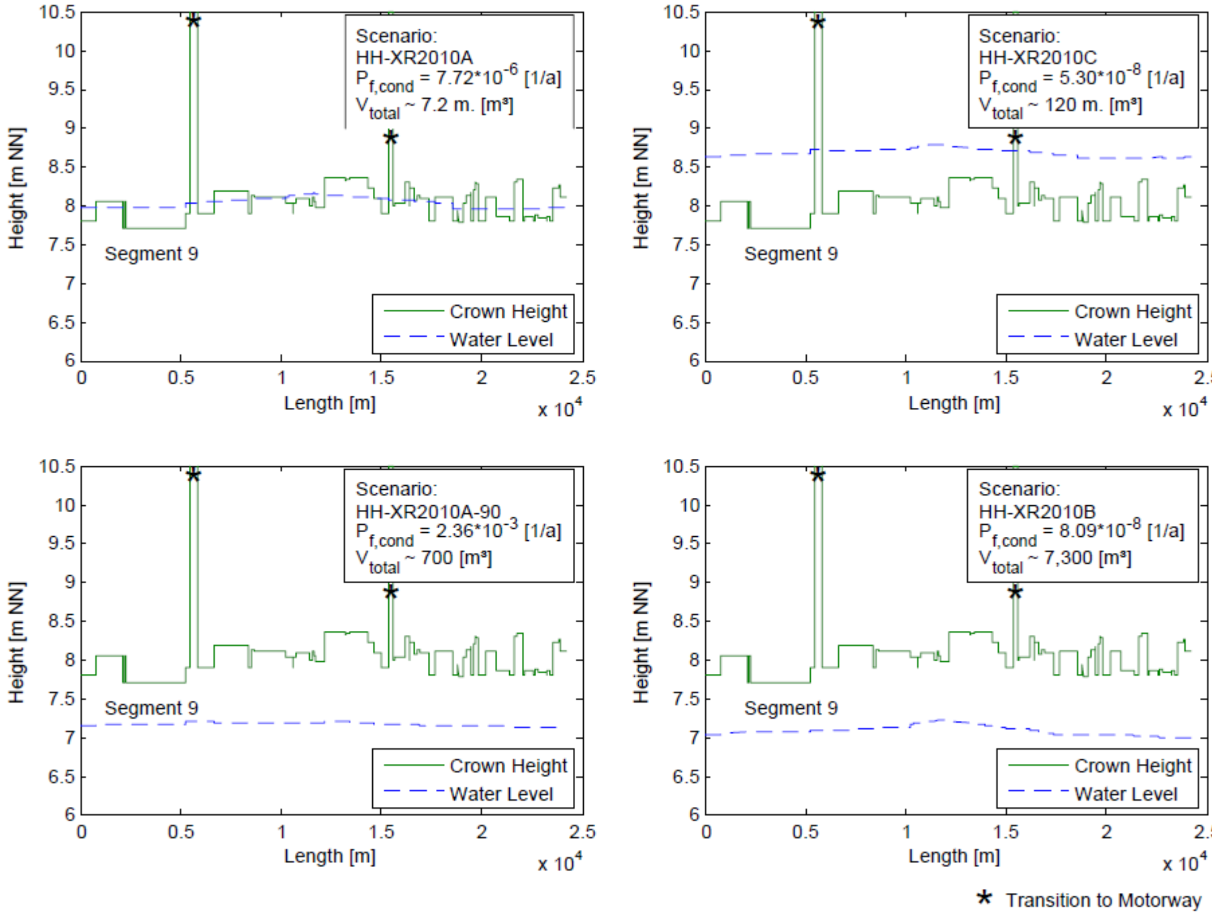

Fig. 6. Crown heights along the flood defense line of Wilhelmsburg, Hamburg, and the associated peak water levels of the extreme storm surge scenarios.

Figure 7 shows the overall discharge summed up along the whole flood defense line passing the defenses and reaching the hinterland. Furthermore, the input time series of the storm surge at the gauge of St. Pauli is given in order to show the characteristics of the storm surge scenarios.

For the analyzed storm surge scenarios HH_XR2010A and HH_XR2010C extreme discharges with total volumes of 7.2 million m^3 and 120 million m^3 (for the whole subarea of Wilhelmsburg) were calculated, respectively. For the storm surge scenarios HH_XR2010A-90 and HH_XR2010B volumes of 700 m^3 and 7,300 m^3 were determined. As it can be seen from the diagrams, the time period of wave overtopping/ overflow varies from 4.25 h to 12.0 h in total. Hence, not only the extreme peaks of the storm surge water level had an influence on the overtopping volumes but also the intensity or fullness of the storm surge curves.

A summary of the results of the maximum overflow rate q_{max} [l/(sm)] and the total overflow volume V_{total} [m^3] for the different storm surge scenarios in Wilhelmsburg, Hamburg, and in Westerland, Sylt, are given in Tables 5 and 6, respectively. In Hamburg the scenarios A and C lead to extreme overflow rates and severe inundation

Naulin, Kortenhaus, Oumeraci: Reliability-Based Flood Defense Analysis in an Integrated Risk Assessment. Coastal Engineering Journal, No. 1 (2015), S. 1540005-[1-35]. S. 1540005-19

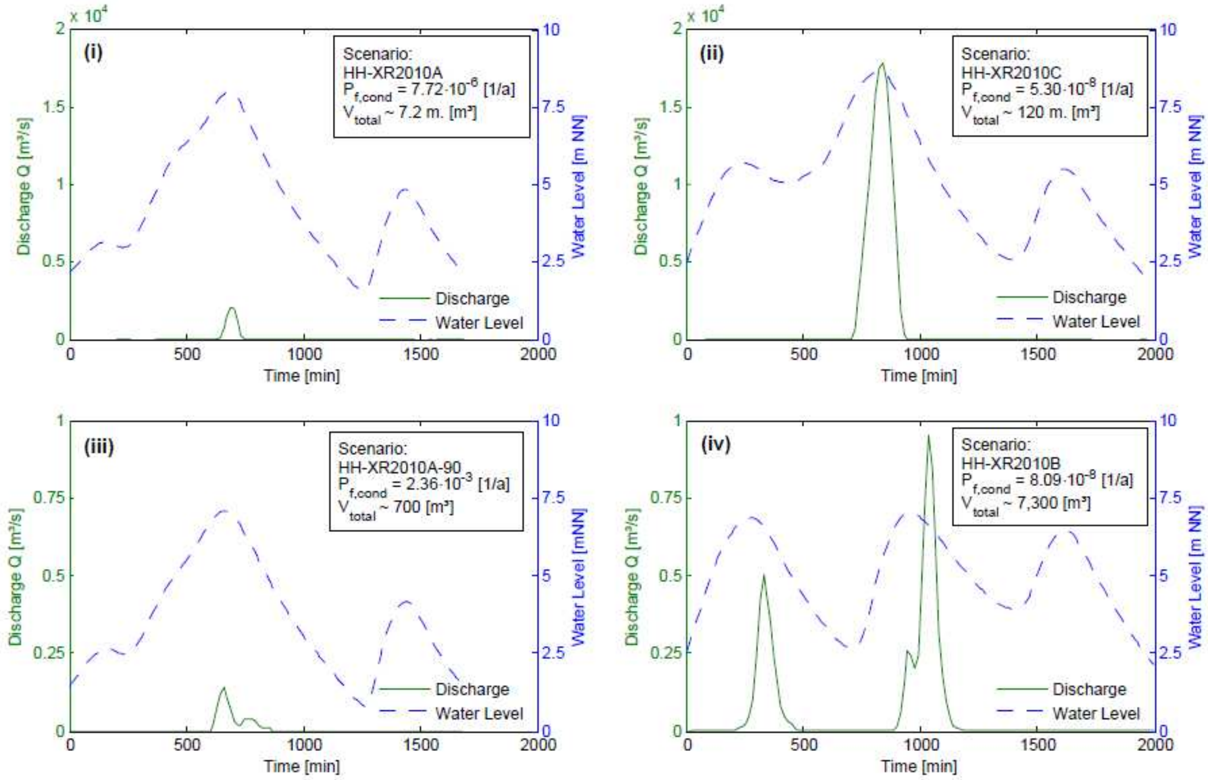

Fig. 7. Total discharges due to wave overtopping/overflow along the flood defense line of Wilhelmsburg, Hamburg, and water levels of the extreme storm surge scenarios at the tide gauge St. Pauli.

Storm surge [Scenario]	q_{max} [l/(sm)]	V_{total} [m³]
HH_XR2010A	660	~7.2 million
HH_XR2010B	2	~7,300
HH_XR2010C	2,260	> 120 million
HH_XR2010A-90	0.5	~700

Table 5. Results of the maximum overflow rate q_{max} [l/(sm)] and total overflow volume V_{total} [m³] for different storm surge scenarios in Wilhelmsburg, Hamburg.

volumes while the scenarios B and A-90 reach rather moderate overtopping rates and volumes. At Sylt the estimated total overflow volumes are rather low. A special feature is observed in Rantumdamm which consists of a first and a second dike line. While at the first dike line significant wave overtopping and overflow may occur, the second dike line seems to prevent the hinterland from flooding.

The overall results show that wave overtopping and overflow may occur at very different locations and at very different times with different durations (see Figs. 6 and 7). Therefore, a change from a time-independent LSE to a time-dependent one is proposed also considering the volumes of water entering the hinterland rather than the discharge over a certain limited stretch of flood defense only. However, this would require a maximum allowable volume of water in the hinterland which needs

Naulin, Kortenhaus, Oumeraci: Reliability-Based Flood Defense Analysis in an Integrated Risk Assessment. Coastal Engineering Journal, No. 1 (2015), S. 1540005-[1-35]. S. 1540005-20

Storm surge [Scenario	Westerland West q_{max} [l/(s ∗ m)]	Rantumdamm (1. dike; 2. dike q = 0) q_{max} [l/(s ∗ m)]	Nössedeich q_{max} [l/(s ∗ m)]	Total V_{total}[m³]
SY_XR2010A	1	730	<0.5	~2,000
SY_XR2010B	<0.5	90	<0.5	~300
SY_XR2010C	<0.5	600	<0.5	~800
SY_XR2010A-95	<0.5	10	<0.5	~0
SY_XR2100A80	7	2,960	13	~25,000
SY_XR2100C80	3	2,760	8	~14,000

Table 6. Results of the maximum overflow rate q_{max} [l/(sm)] and total overflow volume V_{total} [m³] for different storm surge scenarios in Westerland Sylt.

to be derived from the hinterland properties. This issue will be further discussed in Sec. 5.1.

4.3 Breach modeling

This section discusses the results of the breach models for sea dikes and dunes applied to the two pilot sites.

First, for sea dikes, different breach models were applied for the identified weak segments (with a high probability of failure) in order to analyze breach initiation and breach development. The wave overtopping-induced erosion of the inner slope of grassed sea-dikes was simulated first. The breach initiation was modeled using the BREID model which is a numerical model for simulating BREaching of Inhomogeneous sea dikes [Tuan and Oumeraci, 2012]. For this purpose, the effects of different grass conditions were analyzed. Therefore, grass samples of dikes in Hamburg-Wilhelmsburg were taken and laboratory experiments analyzing the root area ratio (RAR) [see e.g. Young, 2005; Ministerie van Verkeer en Waterstaat, 2007; Stanczak et al., 2007] of the grass samples were performed. Good grass conditions were determined following the approach proposed by Tuan and Oumeraci [2012] where grass conditions are linked to different functions of the RAR over the depth of roots in the soil and the results were implemented in the model. The modeling of breach initiation was performed for segment 2 (see Fig. 4). The analysis revealed that even for moderate grass conditions, the grass layer only eroded to a depth of 7.0 cm; i.e. a full breach would not develop under these extreme conditions. It should be noted here that the failure probabilities for inner grass erosion were based on a simple model [Kortenhaus, 2003] which is expected to result in too high failure probabilities. Despite this conservative approach the failure probabilities for the grass erosion were orders of magnitudes lower than any other failure probabilities in the fault tree for these segments.

Second, the full breach development was estimated applying the model of D'Eliso [D'Eliso, 2006] and assuming poor grass conditions. Different dike breach scenarios with breach widths between 18m up to 400m were modeled. The final breach widths

Naulin, Kortenhaus, Oumeraci: Reliability-Based Flood Defense Analysis in an Integrated Risk Assessment. Coastal Engineering Journal, No. 1 (2015), S. 1540005-[1-35]. S. 1540005-21

Storm surge [Scenario]	Dike segment [Name]	Breach width [m]	Volume[m³]	Assumption [-]
HH_XR2010A	Klütjenfelder Hauptdeich (crown height	~400	~72 million	Poor grass condition

	7.80 mNHN; slope 1:3)			
SY_XR2100A80	Rantum Binnendeich (second dike, crown height 3.94 mNHN; slope 1:2,5)	~18	~4 million	breach of first dike line (Rantumdamm)

Table 7. Results of dike breach scenarios model by D'Eliso et al. [2006].

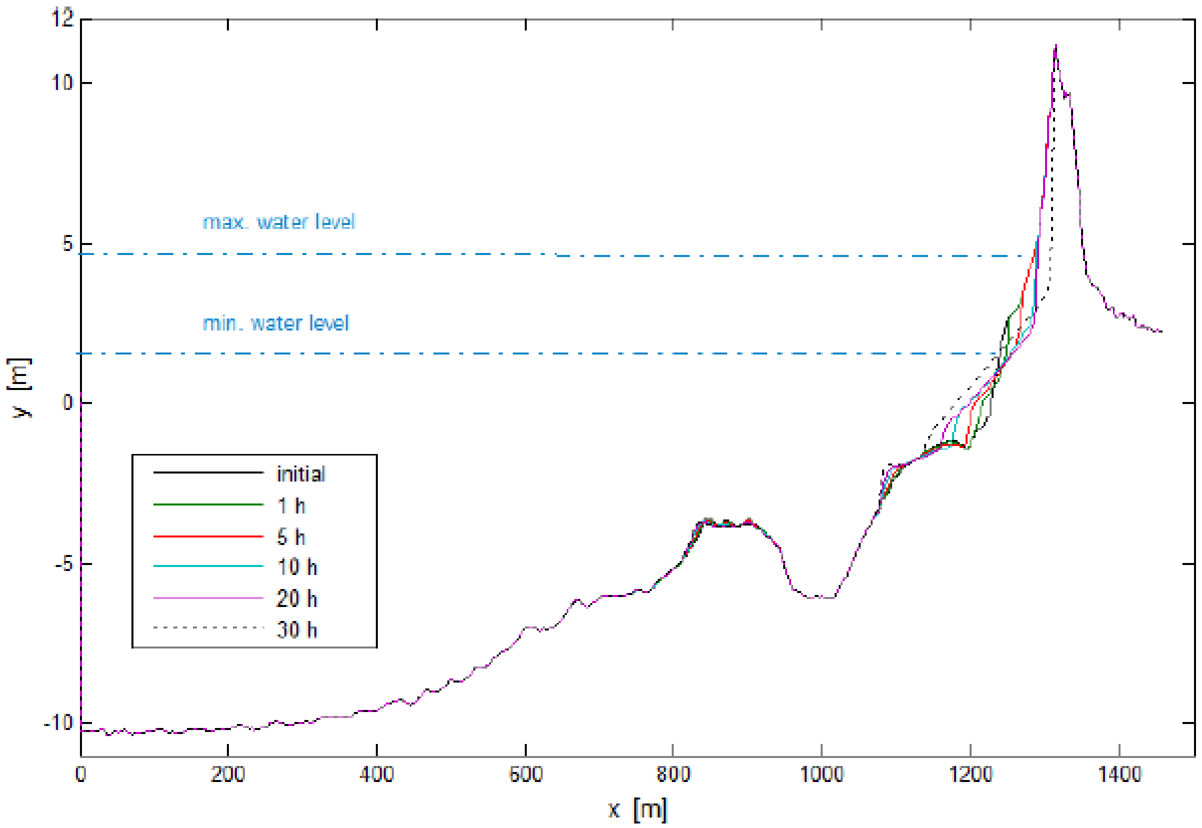

Fig. 8. Initial and erosion profile for a cross-section of a coastal dune in Hörnum, Sylt, for the storm surge scenario SY XR2010C.

and the breach outflow hydrographs were obtained in order to specify the initial conditions of the flood wave at the breach for inundation modeling of the hinterland using the time series of the discharges of the flood defense segments as input parameters [see Ujeyl and Rose, 2015]. In Table 7 the results of the breach modeling are exemplary shown for two storm surge scenarios.

For the coastal dunes at Sylt Island, the results of the reliability analysis revealed that erosion is the relevant failure mechanism for the analyzed storm surge scenarios. Due to the high crown heights of the dunes (12.3–21.5 mNHN) and their large widths of 100m–500m the values for failure probabilities due to overwash [Larson et al., 2009; Nguyen et al., 2006] or a total breach [Coleman et al., 2002] were rather low ($P_f < 1 \cdot 10^{-6}$). For this reason the process of erosion was also simulated by the numerical model Unibest-DE. The results, e.g. for the storm surge scenario

Naulin, Kortenhaus, Oumeraci: Reliability-Based Flood Defense Analysis in an Integrated Risk Assessment. Coastal Engineering Journal, No. 1 (2015), S. 1540005-[1-35]. S. 1540005-22

SY_XR2010C, showed an erosion volume of 57m³/m above the still water level and a decrease in dune width of 25m at the height of 4.5 mNHN (see Fig. 8). Other results were comparable.

These results showed that due to the large dune volume on Sylt Island there was indeed no or very little chance of eroding the dunes during one of the extreme storm surges. Hence, the low values of the failure probability for dune erosion were confirmed. However, it is pointed out that the consequences of the occurrence of chains of extreme storm surge events during one storm surge season were not further investigated. Chains of extreme storm surges could lead to a successive degradation of the dune widths. For the analyzed single extreme storm surge scenarios it was concluded that dune erosion at the west coast of Sylt would not be the relevant failure mechanisms and can be disregarded since its probability is several orders of magnitude lower than those of any of the other key failure mechanisms.

5 Discussion

During the calculation of the failure probabilities of the flood defenses a couple of issues occurred, the details and impacts of which are provided in the following subsections. These issues comprise the time dependency of LSEs (Sec. 5.1), the contribution of segments of different lengths to the overall failure probability (Sec. 5.2), and the so-called length effect (Sec. 5.3).

5.1 Time dependency

This subsection discusses the use of time-dependent LSEs and the resulting failure probabilities as compared to a stationary approach. The overtopping/overflow LSEs are used for the case of Hamburg-Wilhelmsburg to illustrate this approach.

Failure mechanisms of flood defenses are time-dependent processes [Naulin et al., 2011]. The resistance and the loading of the structure vary over time and according to different time scales three general categories can be distinguished (Fig. 9): (a) shortterm, e.g. impacts of storm surges such as wave impacts and wave overtopping, (b) mid-term: seasonal changes, or (c) long term: mean sea level rise, degradation effects.

Figure 9 illustrates the highly unsteady state of both resistance and loading terms of the LSEs which would actually require time-dependent reliability analysis [Buijs et al., 2009].

The approach considered here is exemplarily shown in the following for the failure mechanisms of “wave overtopping” and “overflow”. The common approach for these LSEs is to compare the admissible wave overtopping/overflow rate q_{adm} [$m^3/s/m$] with the actual wave overtopping/overflow rate q [$m^3/s/m$] as follows:

$$z = q_{adm} - q. \tag{3}$$

Naulin, Kortenhaus, Oumeraci: Reliability-Based Flood Defense Analysis in an Integrated Risk Assessment. Coastal Engineering Journal, No. 1 (2015), S. 1540005-[1-35]. S. 1540005-23

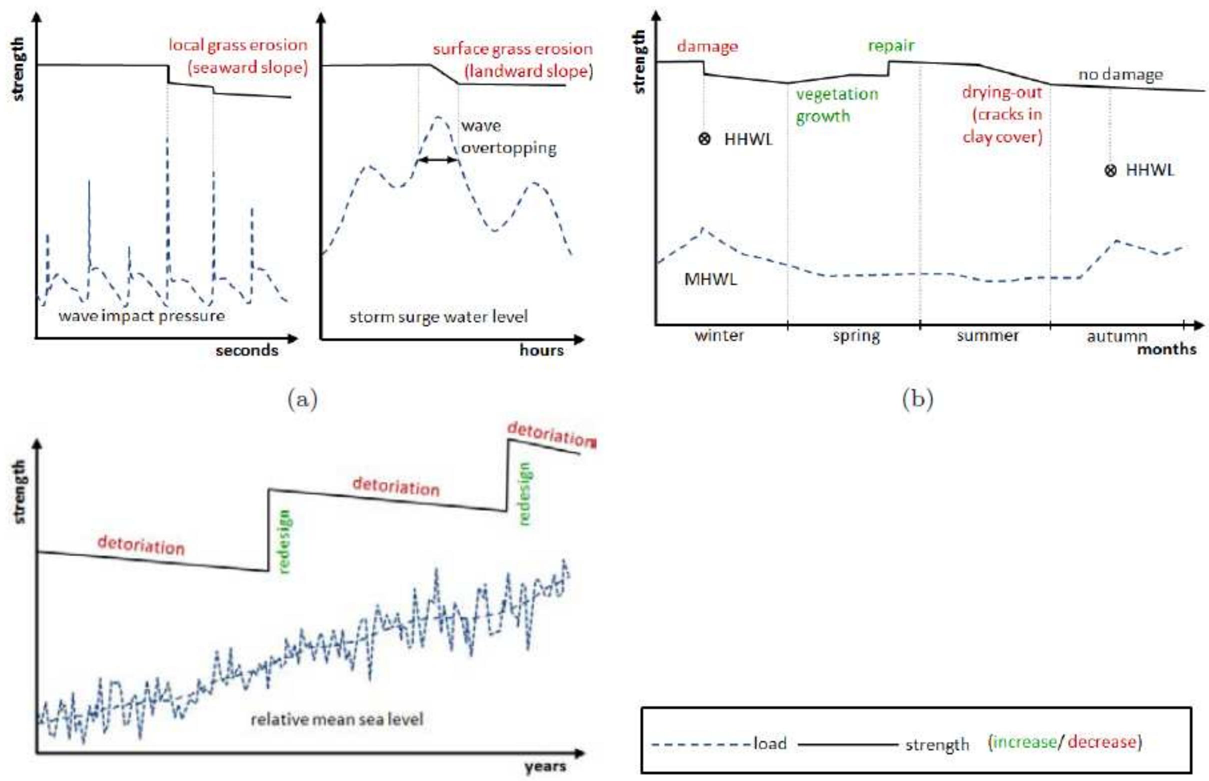

Fig. 9. Time-dependent processes of resistance and loading for different time scales: (a) short term; (b) mid term and (c) long term [Naulin et al., 2012].

The description of the failure mechanisms has been adapted by changing the LSEs for "wave overtopping" and "overflow" from discharges to volumes (Fig. 10):

$$z = V_{adm} - V, \tag{4}$$

where V_{adm} = admissible wave overtopping/overflow volume [m^3] and V = actual wave overtopping/overflow volume [m^3] as follows:

$$V = \sum_{i=1}^{n,m} V_i = q_i \cdot t_i \cdot l_i \tag{5}$$

with q_i = overtopping/overflow discharge of the individual segments, t_i = duration of overtopping/overflow for the segments [s], l_i = length of flood defense segments [m], n = number of time steps [–], m = number of segments [–]. More details of the estimated V can be found in Sec. 4.2 of this paper. Note that the inflow volumes are dependent on time now.

The admissible volume V_{adm} was determined by defining three criteria for the flooded area: (a) the flooded area should remain below 40% of the total area in Wilhelmsburg, (b) the water depth due to flooding should not exceed 1m in areas with buildings, and (c) not more than 40% of the assets in the area should be at risk. Of course these values were taken exemplarilyand are relatively high. However, this

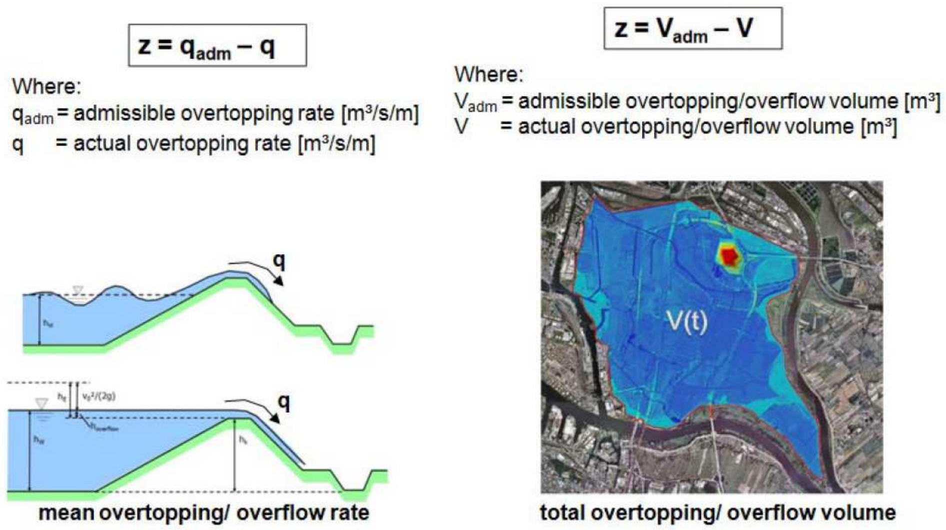

(a) (b)

Fig. 10. LSEs for wave overtopping and overflow comparing (a) discharge rates q and (b) discharge volumes V.

should only demonstrate the principal possibility in defining such a LSE using an admissible volume approach. By using the available inundation modeling scenarios these criteria have led to an admissible volume V_{adm} = 3.8 million m³.

The consideration of time-dependent calculation of volumes instead of discharges with constant parameters has considerable advantages as it represents a better approximation of the time-dependent process, i.e. detailed estimation of overtopping volume. Furthermore, the storage capacity of the hinterland is taken into account, i.e. exceedance of critical overtopping discharge might occur for a short period at the peak of the storm surge, but does not necessarily lead to severe flooding.

For the storm surge scenario HH_XR2010A in Hamburg this modification of the LSE would consequently result in a different flooding probability for the Wilhelmsburg area. The probability can be estimated based on the LSE (Eq. 4) and the relevant estimation of the overtopping/overflow rates in the various segments, also taking into consideration the uncertainties. The flooding probability for this storm surge scenario then results to $P_{f,total}$ = 0.94 for the whole area. Due to the extreme high water levels for the scenario HH_XR2010A this probability is close to what has been estimated by the methods used previously. However, for water levels lower than these extreme levels, such as in scenario HH_XR2010B, the resulting failure probability is $P_{f,total} = 1.2 \cdot 10^{-3}$ (considering admissible volumes) rather than $P_{f,total}$ = 1.0 (considering admissible discharges).

In a second step this overall flooding probability P_f has then to be broken down to individual failure probabilities of the individual segments $P_{f,i}$. This is proposed here by using the contribution of the inflow from the individual segments V_i to

Naulin, Kortenhaus, Oumeraci: Reliability-Based Flood Defense Analysis in an Integrated Risk Assessment. Coastal Engineering Journal, No. 1 (2015), S. 1540005-[1-35]. S. 1540005-25

the overall flooding volume V resulting in a contribution factor f_i for each of the segments as follows:

$$f_i = \frac{V_i}{V} = \frac{q_i \cdot t_i \cdot l_i}{\sum_{i=1}^{n} q_i \cdot t_i \cdot l_i} \tag{6}$$

which would then lead to a local admissible volume for each segment:

$$V_{\mathrm{adm},i} = f_i \cdot V_{\mathrm{adm}} \tag{7}$$

and consequently to a LSE for the individual segment for overflow or overtopping:

$$z = V_{\mathrm{adm},i} - V_i. \tag{8}$$

However, this means that for each segment the ratio between the admissible and the inflowing volume is the same as the one for the overall area, hence resulting in very similar failure probabilities for each of the segments. This is reasonable since the coupling of the various segments by the water level is extremely high, i.e. if there is overtopping in one segment it will overtop in other segments as well. Therefore, in this case, the overall flooding probability can be also taken for all segments where the inflow volume was not zero.

5.2 Importance factor for segment probabilities

The segmentation of the flood defense line has led to segments with different lengths, ranging from about a few tens of meters (like point structures) to very long stretches of several hundreds of meters of dikes. For the pilot site in Hamburg-Wilhelmsburg the shortest segment was 12 m long whereas the longest was 2,800m. This section discusses consequences from these different lengths and proposes a so-called "importance factor" to account for these differences. In case of a complete failure (breach) of a dike segment the different lengths of the segments would lead to a completely different amount of water entering the hinterland.

In case of a gate (point structure with very small width) failing with a high probability of failure under an extreme storm surge this would probably not result in a critical flood situation since there is simply not enough water entering the flood plain. On the other hand, a very long segment with a much lower flooding probability could significantly flood the area due to the width over which the water flows into the hinterland.

Hence, it was concluded that the importance of the segment should be considered for the calculation of the flooding probability. For this purpose, a similar consideration as for the overflow/overtopping calculations in Sec. 5.1 has been performed. The difference here is that the inflow now comes from a whole failure of the flood defense segment rather than from water overtopping it. In addition, the coupling of the segments is less strong since high water levels do not necessarily lead to immediate dike breaches. However, the rest of the approach remains the same in the way that each

Naulin, Kortenhaus, Oumeraci: Reliability-Based Flood Defense Analysis in an Integrated Risk Assessment. Coastal Engineering Journal, No. 1 (2015), S. 1540005-[1-35]. S. 1540005-26

segment probability (without considering wave overtopping/overflow) will be multiplied by a contribution factor for breaching of the segment. This approach needs an additional input parameter indicating the time when the breach develops. It is obvious that the breach will not occur at the beginning of the storm surge, but it is usually extremely difficult to predict the accurate time of the breach. Therefore, it is assumed to occur shortly before the peak of the storm surge which is considered a conservative approach.

In consequence, due to the large inflow volume of water, the volume of water entering the hinterland through a breach in most cases exceeded the admissible flood volume as discussed before. In these cases the influence factor was set to 1.0.

Therefore, the results obtained can be summarized as follows:

1. initial failure probabilities for each segment with probabilities of overflow/ overtopping due to an admissible overtopping discharge of 0.5 l/s/m;
2. an overall flooding failure probability due to time-dependent overflow/ overtopping calculations related to an admissible inflow volume V_{adm};
3. modified failure probabilities for overflow/overtopping for each segment due to an adapted admissible inflow volume $V_{i,adm}$ which are identical to the overall flooding probability in case of very high water levels due to the strong coupling of the segments;
4. weighted failure probabilities for breaching of the flood defense according to their inflow contributions.

If this approach, including the importance factor as shown in the list above, is applied to the XtremRisK storm surge scenarios the results are not so different in case of the very extreme storm surges (HH_XR2010A) since the resulting overtopping failure probabilities are similar in both cases. However, for the pilot-site of Hamburg-Wilhelmsburg and the storm surge scenario HH-

XR2010B the overall flooding probability $P_{f,cond}$ would change from $P_{f,cond} = 1.0$ (without importance factor, see Table 3) to $P_{f,cond} = 1.2 \cdot 10^{-3}$ (including importance factor) which is a significant lower overtopping failure probability. It is therefore suggested here to further elaborate the importance factor approach together with the homogeneous segment division to improve future probability calculations.

5.3 Uncertainties

All probabilistic calculations include uncertainties for the parameters used and the models applied. When uncertainties resulted from measurements they were easy to use, however, in some cases uncertainties are difficult or impossible to assess so that they had to be estimated. This section discusses the consequences of these estimations for the overall failure probabilities of the segments.

Generally, higher uncertainties will always lead to higher failure probabilities. This is always true if for a LSE ($z = R - S$) where the mean value of R is larger

Naulin, Kortenhaus, Oumeraci: Reliability-Based Flood Defense Analysis in an Integrated Risk Assessment. Coastal Engineering Journal, No. 1 (2015), S. 1540005-[1-35]. S. 1540005-27

than the mean value of S. If this is not the case (like in many simulations for overflow and overtopping in this study), it will be the opposite effect. Taking this into account the effect of estimating the uncertainties needed to be quantified.

For this purpose the overtopping simulations using the admissible overflow volume in Hamburg-Wilhelmsburg was taken as an example. Since the estimation of the uncertainties of the admissible overtopping volume itself and the inflowing volume from overtopping calculations and inundation modeling was not really obvious, various estimates were taken, ranging from a coefficient of variation of $\sigma = 25\%$ down to $\sigma = 15\%$. This has changed the results from $P_f = 0.44$ (for 25%) to $P_f = 0.99$ (for 15%) not changing any other simulation parameter at the same time. This difference is still in the same order of magnitude but it suggests higher probabilities occur with lower uncertainties. Therefore, it is crucial to look into uncertainties in some detail and not in all cases higher uncertainties result in more conservative failure probabilities.

5.4 Segment approach and length effect

The "length effect" within reliability analysis has been introduced by CUR [1990] and describes the spatial variability of relevant input parameters along the flood defense line. Further discussions of this matter can be found in Vrijling and Van Gelder [2002] and Buijs [2003] which used different approaches to define segments of the flood defense line. The former proposed segments of equal length and introduced correlation matrices to account for the correlation of parameters along the defense line whereas the latter proposed segment lengths which assumed homogeneous conditions within one segment and fully independent parameters from one segment to the next. This latter approach was also adopted in this study. This section seeks to discuss the consequences from this approach with respect to the calculated overall flooding probability and to give some proof why this approach is believed to be the best suitable here.

Following the above, one of the key assumptions for the pathway analysis in this paper was that the different segments of the flood defense lines are independent from each other and can be treated as a series system. This means that the whole flood defense system can be calculated from a fault tree approach using OR-gates (similar to the fault tree for the failure modes of one segment) and can therefore be estimated as follows [see e.g. Kortenhaus, 2003]:

$$P_{f,\text{system,indep.}} = 1 - \prod_{i=1}^{n} (1 - P_i) \approx \sum_{i=1}^{n} P_i \quad , \tag{9}$$

where $P_{f,system,indep.}$ is the failure probability of the overall system (e.g. the dike ring), n is the number of segments in the system and P_i is the failure probability of the individual segment. The approximation by the sum of the individual failure

probabilities can obviously only work for small P_i since otherwise the sum may get larger than 1.

Assuming full dependency of all segments in a series system on the other hand means that the system failure probability equals the maximum of all individual segment probabilities such as:

$$P_{f,system,dep.} = \max(P_i) \tag{10}$$

which has been validated in the calculation of the overtopping probabilities in this study for very high water levels (Scenario HH_XR2010A). Dike ring areas can however be very different (consider e.g. the 40 km long coast along Sylt Island and the ring-like area in Hamburg-Wilhelmsburg). However, the assumption taken in this study was to determine “homogeneous” segments. The segments are regarded as principally independent from each other. From what has been mentioned above (Eq. (10)), this means that the failure probability $P_{f,system}$ will increase with an increasing number of segments (for the same overall length of the dike ring defenses) or with a decreasing lengths of segments. The effect of a wrong segmentation of the flood defense line, which may for example result from insufficiently defined criteria or data scarcity, has therefore to be estimated.

Taking again the case of Hamburg-Wilhelmsburg and storm surge scenario HH_XR2010A, the number of segments has been varied and the following results were achieved:

- Considering the overtopping/overflow LSE (with admissible overtopping discharge of 0.5 l/s/m), the overall flooding probability will remain 1.0, regardless of the number of segments. This is due to the fact that the overall failure probability will also be P_f = 1.0 if any single segment results in $P_{f,i}$ = 1.0.
- Ignoring the overtopping/overflow LSE the overall flooding probability was P_f = 0.44. Increasing the number of segments by a factor of 2 and 3 rather than 1 (with identical failure probabilities of these segments) would result in P_f = 0.68 and P_f = 0.82, respectively.
- Still ignoring the overtopping/overflow LSE and bringing together all dike segments (leaving all other types of flood defenses as separate segments) resulted in P_f = 0.34.

It can be seen from this comparison that in case of failure probabilities of the flood defense line segments where $P_{f,i}$ = 1 no length effect needs to be considered. In all cases where the segments are strongly coupled (as in this study by the extreme water levels), the length effect can be ignored since the overall flooding probability should be calculated by the inflow volume approach as described in Sec. 4.2. For all other cases investigated here the aforementioned calculations suggest that the results may change from about 80% to 190% of the initial calculations.

Although the latter variations are not small, they are still in the same range or smaller than the effect of changing the uncertainties in these simulations as discussed

Naulin, Kortenhaus, Oumeraci: Reliability-Based Flood Defense Analysis in an Integrated Risk Assessment. Coastal Engineering Journal, No. 1 (2015), S. 1540005-[1-35]. S. 1540005-29

in the previous section. However, segmentation should be carefully performed, but given the previous simulations, the approach selected here was believed to be the best available approach rather than splitting the defense line into segments of equal length and estimating their correlations.

6 Summary and Concluding Remarks

The German research project XtremRisK has developed methods for an integrated flood risk assessment for extreme storm surges where the city of Hamburg serves as a pilot site for an estuarine urban area, and the Sylt Island serves as a pilot site for an open coast. Subproject 2 (SP 2) of XtremRisK has dealt with reliability analyzes and breach modeling of coastal and estuarine flood defenses the results of which are described in this paper.

Within the reliability analysis, software tools were developed for the identified main linear flood defense elements of the pilot sites, i.e. estuary/sea dikes; coastal dunes and flood defense walls/sea walls. Overall, 35 LSEs were considered and up to more than 80 input parameters were determined for the flood defenses. In addition, more detailed wave overtopping/overflow calculations and breach modeling were performed to determine discharges as initial conditions of the flood wave propagation into the hinterland.

The methods were applied to the pilot sites of Hamburg and Sylt Island resulting in conditional failure probabilities for different extreme storm surge scenarios. These storm surges comprised very high water levels leading to very high failure probabilities for wave overtopping and overflow of up to $P_f = 1.0$. However, the probabilities of full dike breaches were found to be rather low (typical range of $P_f = 1.0 \cdot 10^{-4}$) where segments with higher probabilities ($P_f = 1.0 \cdot 10^{-2} – 1.0 \cdot 10^{-3}$) were identified as potential weak points for breaching.

More detailed time-dependent calculations of wave overtopping and overflow have shown that severe flooding occurred for the analyzed storm surge scenarios. The results of the breach modeling pointed out that a breach could be initiated at the landward side but would not fully develop for current scenarios. A full breach would only develop under the assumption of poor grass conditions.

In discussing some of the results of this study, methods were suggested in order to consider the time dependence of failure mechanisms in terms of the unsteady conditions of the storm surge, e.g. by changing the LSEs for “wave overtopping” and “overflow” from discharges to volumes. Calculations have shown that this would lead to a significant reduction of the flooding probabilities in case of less extreme water levels (case of scenario HH_XR2010B). Furthermore, some considerations of the length effects which might result from the segmentation of the flood defense line have been performed. The results show that the approach implemented in this study is believed to be the most accurate and yet still conservative.

Naulin, Kortenhaus, Oumeraci: Reliability-Based Flood Defense Analysis in an Integrated Risk Assessment. Coastal Engineering Journal, No. 1 (2015), S. 1540005-[1-35]. S. 1540005-30

However, future challenges remain, e.g. a systematic analysis of “point structures” where human and organizational errors may contribute to higher failure probabilities. In addition, weak points with potential increase of failure probabilities such as transitions between different types of flood defense elements or damages due to burrowing animals have to be further investigated.

Acknowledgments

The XtremRisK project was funded by the German Federal Ministry of Education and Research (BMBF) through the project management of Projektträger Jülich (PTJ) under the grant number

03F043B. Data sets were kindly provided by the Shipping Administration of the Federal Government (WSA), the Government-Owned Company for Coastal Protection, National Parks and Ocean Protection (LKN), HPA Hamburg (Hamburg Port Authority) and LSBG Hamburg (Agency of Roads, Bridges and Waters, Hamburg), the support of which is gratefully acknowledged here.

Furthermore, the very good and constructive collaboration in between the XtremRisK partners is very gratefully acknowledged. Without this team spirit and always useful feedback and support from all partners the project would not have achieved its objectives.

Appendix A. Pilot Site Details

A brief overview of the pilot sites used for the reliability analysis in this paper is provided in Sec. 3 of this paper. This Appendix provides more details regarding the two pilot sites and how data for the risk pathways were assessed.

In Hamburg there is a strong influence of the tidal dynamics of the North Sea with a mean high tide of 2.1m above Normalhöhennull (NHN, reference datum for water level in Germany). The current design water level is 7.30 mNHN at the tide gauge of St. Pauli, Hamburg. Estuary dikes, flood defense walls and a huge number of "point structures" to close the openings in the harbor area in case of a storm surge are found as main flood defense elements in Hamburg.

At Sylt the mean high tide is about 1.0 mNHN and the current design water level is 4.50 mNHN. Since wind and wave attack are predominantly originating from westerly directions, there is a severe wave loading on the west side of the island. Coastal dunes are mainly used as flood defenses on the west side of the island. Moreover, especially in Westerland, concrete revetments and sea walls have been built. The east side of the island is protected by sea dikes, flood walls and revetments.

Overall, there was a large amount of data available but with very different levels of details for the various areas and segments. For some dike segments detailed crosssections and geotechnical reports with soil parameters were available. For other

dike segments only the crown height was known. Therefore, the data had to be homogenized and simplified for most of the segments. For this, the following steps were performed:

Using this data basis, which was managed in a geographical information system (GIS), the flood defense line of each subarea was then divided into homogeneous segments with similar characteristics such as type of structure, geometric parameters and geotechnical parameters. In general more than 30 geometric parameters could be identified in order to describe the cross-section of the structure whereof the major parameters such as crown height, the seaward slope, and the width of the crown

				Crown height	
Subarea	Structure	Number [-]	Length [-]	min [m NHN]	max [m NHN]
Hamburg					
Wilhelmsburg	Dike	71	19,336	7.70	10.60
	Flood wall	7	4,141	7.77	10.60
	Point structures	16	-	7.80	8.22
	Total	**94**	**23,477**	**7.70**	**10.60**
Polder Ham-burg Süd	Flood wall	42	2,710	7.50	7.50
	Point structures	43	-	7.50	7.50
	Total	**85**	**2,710**	**7.50**	**7.50**
City center	Flood wall	8	1,098	7.60	7.80
	Point structures	5	-	7.50	7.50
	Total	**13**	**1,098**	**7.50**	**7.80**
Sylt					
Hörnum	dune	4	762	4.10	5.84
	Dune/tetrapods	4	375	4.20	4.98
	Dune beach path	19	3,766	6.50	17.70
	Revetment	3	724	7.72	13.96
	Dike with bulk-	14	412	8.12	16.06

	head				
	Flood wall*	4	496	3.90	4.25
	Total	**48**	**6,535**	**3.90**	**17.70**
Westerland	Dune	17	3,314	13.17	21.47
	Dune/tetrapods	9	1,411	12.96	20.97
	Dune beach path	10	193	12.73	19.35
	Sea wall/revetment	10	1,020	10.13	14.94
	Sea wall	7	494	9.78	13.69
	Dike (incl. second dike line)	32	13,808	3.82	7.44
	Point structures*	4	-		
	Total	**89**	**20,241**	**3.82**	**21.47**

Table A.1. Results of the segmentation of the flood defense line for the different subareas of the pilot sites Hamburg and Sylt.

Naulin, Kortenhaus, Oumeraci: Reliability-Based Flood Defense Analysis in an Integrated Risk Assessment. Coastal Engineering Journal, No. 1 (2015), S. 1540005-[1-35]. S. 1540005-32

represent some of the main selection criteria. Although up to over 40 geotechnical parameters were required as input parameters the available data was rather poor. However, for dikes some data on the thickness of the clay layer and the clay and sand properties could be investigated. Moreover, the hydraulic conditions such as water level and wave conditions (wave height and wave period at the toe of the structure) were also considered for the subdivision.

An overview of the results of the analysis of the flood defense line of the different subareas of the pilot sites in Hamburg and Sylt is given in Table A.1. For each subarea of the pilot sites, the flood defense type, the number and length of the identified segments and their crown heights are summarized.

The subareas of Hamburg-Wilhelmsburg, Polder Hamburg Süd and the subzone of the city centre are protected by flood defense lines with lengths of 23.8, 2.7 and 1.1 km which were divided into 94, 85, and 13 segments, respectively.

The investigated subareas of Sylt Island included 6.5 km of flood defense line divided into 48 segments in Hörnum and 20.2 km divided into 89 segments in Westerland.

Estuary and sea dikes, coastal dunes and flood defense walls/sea walls were identified as main linear flood defense elements. Furthermore, there was a great variety of so called “point structures” such as sluices, barriers and gates. Particularly, a huge number of gates were found in the polder Hamburg Süd in the harbor of Hamburg.

References

Allsop, W., Kortenhaus, A., Morris, M., Buijs, F., Hassan, R., Young, M., Doorn, N., van der Meer, J., Van Gelder, P., Dyer, M., Redaelli, M., Utily, S., Visser, P., Bettess, R., Lesniewska, D. & ter Horst, W. [2007] “Failure mechanisms for flood defence structures, FLOODsite — Integrated Flood Risk Analysis and Management Methodologies,” Report no. T04-06-01, 211 pp.

Apel, H., Merz, B. & Thieken, A. H. [2009] “Influence of dike breaches on flood frequency estimation,” Comput. Geosci. 35(5), 907–923.

Apel, H., Thieken, A. H., Merz, B. & Blöschl, G. [2004] “Flood risk assessment and associated uncertainty,” Nat. Hazards Earth Syst. Sci. 4(2), 295–308.

Bardet, J. P. & Tobita, T. [2002] “A practical method for solving free-surface seepage problems,” Comput. Geotech. 29(6), 451–475.

Bishop, A. W. [1955] “The use of slip circle in the stability analysis of slopes,” Geotechnique 5, 7–17.

Bleck, M., Oumeraci, H. & Sch¨uttrumpf, H. [2000] “Combined wave overtopping and overflow of dikes and seawalls,” in Proc. 27th Int. Conf. Coastal Engineering, July 16–21, 2000, Sydney, Australia, Vol. 27, Poster Paper (ASCE, USA).

Bligh, W. G. [1910] “Dams, barrages and weirs on porous foundations,” Eng. News 63/64, 708.

Buijs, F. A. [2003] Reliability Analysis of the Caldicot Levels’ Flood Defense System by Using Dutch Reliabiltiy Methods for Flood Defences (Technical University of Delft, Delft, The Netherlands), 127 pp.

Buijs, F., Hall, J. W., Sayers, P. B. & Van Gelder, P. H. A. J. M. [2009] "Time-dependent reliability analysis of flood defences," Reliab. Eng. Syst. Safe. 94(12), 1942–1953.

Burzel, A., Dassanayake, D. & Oumeraci, H. [2015] "Spatial modeling of tangible and intangible losses in integrated coastal flood risk analysis," Coast. Eng. J. 57(1), 1540008.

Naulin, Kortenhaus, Oumeraci: Reliability-Based Flood Defense Analysis in an Integrated Risk Assessment. Coastal Engineering Journal, No. 1 (2015), S. 1540005-[1-35]. S. 1540005-33

Coleman, S. E., Andrews, D. P. & Webby, M. G. [2002] "Overtopping breaching of noncohesive homogenous embankments," J. Hydraul. Eng. 128(9), 829–838.

CUR [1990] "Probabilistic design of flood defences," Centre for Civil Engineering Research, Codes and Specification, Vol. 141 (Gouda, The Netherlands), 154 pp.

Dassanayake, D., Burzel, A. & Oumeraci, H. [2015] "Methods for the evaluation of intangible flood losses and their integration in flood risk analysis," Coast. Eng. J. 57(1), 1540007.

D'Eliso, C., Oumeraci, H. & Kortenhaus, A. [2006] "Breaching of coastal dikes induced by wave overtopping," in Proc. 30th International Conference Coastal Engineering (ICCE), San Diego, Vol. 3 (USA, ASCE), pp. 2844–2856. De Mello, V. F. [1975] "Some lessons from unsuspected, real and fictitious problems in earth dam engineering in Brazil," in Proc. 6th Regional Soil Mechanics and Foundation Engineering Conference for Africa, Durban, South Africa, Vol. 1 (Balkema, Rotterdam, The Netherlands), pp. 285–304.

DIN 1054 [1996] DIN 1054 : Sicherheitsnachweise im Erd- und Grundbau (Beuth Verlag, Berlin, Germany), pp. 109–191. DIN 4084 [1983] DIN 4084 : Gelände- und Böschungsbruchberechnungen (Beuth Bauverlag, Berlin, Germany), pp. 266–301.

DIN 19712 [1997] Flussdeiche (Beuth Verlag GmbH, Berlin, Germany).

EurOtop [2007] "European overtopping manual," in Die Küste. Archiv f˙ur Forschung und Technik an der Nord- und Ostsee, eds. Pullen, T., Allsop, N. W. H., Bruce, T., Kortenhaus, A., Schüttrumpf, H. & Van der Meer, J. W., Vol. 73 (Westholsteinische Verlagsanstalt, Heide), www.overtopping-manual.com, 178 pp.

Gönnert, G. & Gerkensmeier, B. [2015] "A multi-method approach to develop extreme storm surge events to strengthen the resilience of highly vulnerable coastal areas," Coast. Eng. J. 57(1), 1540002.

Gouldby, B., Sayers, P., Mulet-Marti, J., Hassan, M. & Benwell, D. [2008] "A methodology for regional-scale flood risk assessment," Proc. Inst. Civil Eng. Water Manag. 161(3), 169–182.

Hall, J. W., Dawson, R. J., Sayers, P. B., Rosu, C., Chetterton, J. B. & Deakin, R. [2003] "A methodology for national-scale flood risk assessment," Proc. Inst. Civil Eng. Water Mar. Eng., Vol. 156(3), pp. 235–247.

Heffernan, J. E. & Tawn, J. A. [2004] "A conditional approach for multivariate extreme values (with discussion)," J. Roy. Statist. Soc. Ser. B 66(3), 497–546.

Hussaarts, M., Vrijling, J. K., van Gelder, P. H. A. J. M., de Looff, H. & Blonk, C. [1999] "The probablistic optimisation of the revetment on the dikes along the Frisian coast," in Proc. Coast. Structures'99, Santander, Spain, Vol. 1 (Balkema Publishers, Rotterdam, The Netherlands), pp. 325–330.

INFRAM [2000] "Rudimentaire opzet erosiemodel dijken," Internal Report, INFRAM, Zeewolde, The Netherlands, 8 pp.

IPCC [2013] "Climate change 2013: The physical science basis," Working Group I Contribution to the Fifth Assessment Report of the Intergovermental Panel on Climate Change, Intergovermental Panel on Climate Change (IPCC) (Genf, Schweiz), 1552 pp.

Klein Breteler, M. [1994] "Case study Noord Schuddeland — betrouwbaarheidsfuncties voor dijkbekledingen inclusief reststerkte," WL/Delft Hydraulics, Report H1687 (Delft, The Netherlands).

Kortenhaus, A. [2003] "Probabilistische methoden für nordseedeiche," Ph.D. thesis, Dissertation, Fachbereich Bauingenieurwesen, Leichtweiß-Institut für Wasserbau, Technische Universit ¨at Braunschweig, Braunschweig, Germany, 154 pp.

Kortenhaus, A. & Oumeraci, H. [2002] "Probabilistische Bemessungsmethoden für Seedeiche," Berichte Leichtweiß-Institut für Wasserbau, Technische Universität Braunschweig, Vol. 877 (Braunschweig, Germany), 205 pp.

Lamb, R. et al. [2010] "A new method to assess the risk of local and widespread flooding on rivers and coasts," J. Flood Risk Manag. 3(4), 323–336.

Naulin, Kortenhaus, Oumeraci: Reliability-Based Flood Defense Analysis in an Integrated Risk Assessment. Coastal Engineering Journal, No. 1 (2015), S. 1540005-[1-35].	S. 1540005-34

Lane, E. W. [1935] Security from under-seepage — Masonry dams on earth foundations," Trans. Amer. Soc. Civil Eng. 100, 1235–1351.

Larson, M., Donnelly, C., Jimenez, J. A. & Hanson, H. [2009] "Analytical model of beach erosion and overwash during storms," Proc. Inst. Civil Eng., Mar. Eng. 162(3), 115–125.

Mai Van, C. [2010] "Probabilistic design of coastal flood defences in Vietnam," Ph.D. thesis, Technical University of Delft, Delft, Netherlands, 245 pp.

Merz, B. [2006] Hochwasserrisiken. Grenzen und Möglichkeiten der Risikoabschätzung (Schweizerbart'sche Verlagsbuchhandlung, Stuttgart), 334 pp.

Ministerie van Verkeer en Waterstaat [2007] "Voorschrift Toetsen op Veiligheid, primaire waterkeringen," Ministry of Transport, Public Works and Water Management, Vol. VTV, 472 pp.

Naulin, M., Kortenhaus, A. and Oumeraci, H. [2011] in Vogt, Schuppener, Straub & Bräv (eds), "Reliability analysis and breach modelling of coastal and estuarine flood defences," in Proc. 3rd Int. Symp. Geotechnical Safety and Risk (ISGSR2011) (Munich, Gemany).

Naulin, M., Kortenhaus, A. & Oumeraci, H. [2012] "Reliability analysis and breach modelling of flood defences in an integrated risk analysis — results of the XtremRisK project, in Proc. 2nd European Conf. Flood Risk Management, FLOODrisk2012 (CRC Press, Rotterdam, The Netherlands).

Nguyen, X. T., Larson, M. & Donelly, C. [2006] "A new empirical formula for coastal overwash," Vietnam — Japan Estuary Workshop, Hanoi, Vietnam, pp. 60–65.

Oumeraci, H., Kortenhaus, A., Allsop, W., de Groot, M., Crouch, R., Vrijling, H. and Voortman, H. [2001] "Probabilistic Design Tools for Vertical Breakwaters. The Netherlands: Swets & Zeitlinger B.V., 320 pp.

Oumeraci, H., Kortenhaus, A., Burzel, A., Naulin, M., Dassanayake, D., Jensen, J., Wahl, Th., Mudersbach, C., Gönnert, G., Gerkensmeier, B., Fröhle, P. & Ujeyl, G. [2015] "XtremRisK — Integrated flood risk analysis for extreme storm surges at open coasts and in estuaries: Methodology, key results and lessons learned," Coast. Eng. J. 57(1), 1540001.

Peter, G. [2005] Überfälle und Wehre Grundlagen und Berechnungsbeispiele (Vieweg Verlag, Wiesbaden).

Richwien, W. & Weißmann, R. [1999] "Quantifizierung der Sicherheitsreserven von Seedeichen bei Wellenüberlauf," Abschlußbericht. Institut für Grundbau und Bodenmechanik, Universität und Gesamthochschule Essen, Vol. Teil IV (Essen, Germany), 55 pp.

Scheuermann, A. [2005] "Instationäre Durchfeuchtung quasi-homogener Erddeich (Heft 164)," Ph.D. thesis, Universität Karlsruhe, Institut für Bodenmechanik und Felsmechanik, Karlsruhe, Germany.

Schüttrumpf, H., Lennartz, G., Hill, P., Schumann, A. & Wille, B. [2009] "Entwicklung eines risikobasierten Entscheidungshilfesystems zur Identifikation von Schutzmaßnahmen bei extremen Hochwasserereignissen — REISE: Abschlussbericht zum Verbundvorhaben innerhalb der BMBF-Förderaktivität rimax, RIMAX — Risikomanagement extremer Hochwasserereignisse," Aachen, 292 pp.

Schwartz, M. L. (ed.) [2005] Encyclopedia of Coastal Science (Springer, Dordrecht, The Netherlands), 1086 pp.

Sellmeijer, J. B. [1988] "On the mechanics of piping under impervious structures," Ph.D. thesis, LGM mededelingen/Laboratorium voor Grondmechanica, Stichting Waterbouwskundig Laboratorium, LGM, Delft, The Netherlands, 43 pp.

Sönnichsen, U. & Moseberg, J. [1997] Wenn die Deiche brechen: Sturmfluten und Küstenschutz an der schleswig-holsteinischen Westküste und in Hamburg, 2nd edn. (Husum Druck- und Verlagsgesellschaft, Germany), 128 pp.

Stanczak, G. & Oumeraci, H. [2012] "Model for prediction of sea dike breaching initiated by breaking wave impact," Natural Hazards 61(2), 673–687. Stanczak, G., Oumeraci, H. & Kortenhaus, A. [2007] "Laboratory tests on the erosion of clay revetment of sea dike with and without a grass cover induced by breaking wave impact, FLOODsite — Integrated Flood Risk Assessment and Management Methodologies," Vol. 935, Task 4 (Braunschweig, Germany), 40 pp.

Naulin, Kortenhaus, Oumeraci: Reliability-Based Flood Defense Analysis in an Integrated Risk Assessment. Coastal Engineering Journal, No. 1 (2015), S. 1540005-[1-35].	S. 1540005-34

Steenbergen, H. M. G. M. & Vrouwenvelder, A. C. W. M. [2003]: "Deel A: Mechanismenbeschrijvingen," Theoriehandleiding PC-Ring, Versie 4.0, TNO Bouw rapport 2003-CI-R0020.

Steetzel, H. J. [1993] "Cross-shore transport during storm surges," Ph.D. thesis, Den Haag, The Netherlands, 242 pp.

Tayel, M. & Oumeraci, H. [2015] "A hybrid approach using hydrodynamic modelling and artificial neural networks for extreme storm surge prediction," Coast. Eng. J. 57(1), 1540004.

TNO [1998] "Case study GroFriland," report prepared for TAW.

Tuan, T. Q. & Oumeraci, H. [2010] "A numerical model of wave overtopping on seadikes," Coast. Eng. 57, pp. 757–772.

Tuan, T. Q. & Oumeraci, H. [2012] "Numerical modelling of wave overtopping-induced erosion of grassed inner sea-dike slopes," Nat. Hazards 63(2), 417–447.

Ujeyl, G. & Rose, J. [2015] "Estimating direct and indirect damages from storm surges: The case of Hamburg-Wilhelmsburg," Coast. Eng. J. 57(1), 1540006.

Van der Meer, J. W. [1998] "Application and stability criteria for rock and artificial units," in Dikes and Revetments, ed. Pilarczyk, K. W. (A. A. Balkema, Rotterdam/Brookfield), pp. 191–215.

Van Gelder, P. H. A. J. M., Buijs, F., Van, C. M., ter Horst, W. L. A., Kanning, W., Nejad, M., Gupta, S., Shams, R., Van Erp, N., Gouldby, B., Kingston, G., Sayers, P., Wills, M., Kortenhaus, A. & Lambrecht, H.-J. [2008] "Reliability analysis of flood sea defence structures and systems, FLOODsite — Integrated flood risk assessment and management methodologies," Report T07-08-01, Task 7, 118 pp.

Verheij, H. J. [1997a] "Marsroute TAW — case study Centraal Holland," WL/ Delft Hydraulics, Report Q2229, Delft, The Netherlands.

Verheij, H. J. [1997b] "Marsroute TAW — case study Noord-Beveland," WL/ Delft Hydraulics," Report Q2229, Delft, The Netherlands.

Voortman, H. G. [2002] "Risk-based design of large-scale flood defence systems," Ph.D. thesis, Delft University of Technology, Delft, The Netherlands, 216 pp.

Vorogushyn, S. [2009] "Analysis of flood hazard under consideration of dike breaches," Ph.D. thesis, University of Potsdam, Faculty of Mathematics and Natural Sciences, Potsdam, Germany, 165 pp.

Vorogushyn, S., Merz, B., Lindenschmidt, K. E. & Apel, H. [2010] "A new methodology for flood hazard assessment considering dike breaches," Water Resources Res. 46, 17 pp.

Vrijling, J. K. & van Gelder, P. H. A. J. M. [2002] Probabilistic Design in Hydraulic Engineering (Technical University Delft, CTWA 5310 (F30)).

Wahl, T., Mudersbach, C. & Jensen, J. [2015] "Statistical assessment of storm surge scenarios within integrated risk analyses," Coast. Eng. J. 57(1), 1540003.

Weijers, J. B. A. & Sellmeijer, J. B. [1993] "A new model to deal with the piping mechanism," in Filters in Geotechnical and Hydraulic Engineering, ed. Brauns, H. S. E. (Balkema, Rotterdam, The Netherlands), pp. 349–355.

Wyncoll, D. & Gouldby, B. [2013] "Integrating a multivariate extreme value method within a system flood risk analysis model," J. Flood Risk Manag., doi: 10.1111/jfr3.12069.

Young, M. J. [2005] "Wave overtopping and grass cover layer failure on the inner slope of dikes," Ph.D. thesis, UNESCO-IHE, Institute for Water Education, Delft, The Netherlands, 89 pp.

Zesch, R., Saucke, U., Triantafyllidis, T. & Bieberstein, A. [2007] "Probabilistisches Bemessungskonzept für das Versagen von Flussdeichen unter Berücksichtigung geotechnischer Gegebenheiten," in Verständnis, Vorsorge und Bewältigung von Naturkatastrophen, Abschlusssymposium 2007, Graduiertenkolloeg "Naturkatastrophen," ed. Senitz, S. (Universitätsverlag Karlsruhe, Universität Karlsruhe (TH), Germany), pp. 113–122.